OPTOMECHANICS OF CAVITY DRIVEN NANOPARTICLES

By

Joel T. Rubin

A dissertation submitted to the Graduate Faculty in Physics in partial fulfillment of the requirements for the degree of Doctor of Philosophy, The City University of New York

2012

This manuscript has been read and accepted for the

Graduate Faculty in Physics in satisfaction of the

dissertation requirement for the degree of Doctor of Philosophy

Chair of Examining Committee: Lev Deych

Date _____ Signature _____

Executive Officer: Steven Greenbaum

Date _____ Signature _____

Supervisory Committee:

Igor Kuskovsky

Alexander Lisyansky

Lev Murokh

Mikhail Sumetsky

ABSTRACT

OPTOMECHANICS OF CAVITY DRIVEN NANOPARTICLES

By

Joel T. Rubin

Adviser: Professor Lev Deych

The subject of this thesis is the optomechanical interaction of a spherical high-Q microresonator and a subwavelength particle, which, at optical wavelengths, corresponds to a size on the order of nanometers. After a review of the basic theory of spherical resonators and multi-sphere scattering, the full self-consistent electromagnetic field of the coupled resonator-particle system is derived. The particle-induced frequency shift and broadening is calculated by examining the poles of the scattering coefficients of the resonator. The force exerted on the particle by the field is determined via the Maxwell stress tensor, and is found to be in general non-conservative. From the force, the trajectories of the particle positioned outside the resonator are investigated. The relationship between frequency shift and the conservative and non-conservative components of the force is found to differ from the well-known formulas for the "gradient" and "scattering" force, which are commonly derived by neglecting the modification of the resonator field by the particle. The key aspects of this difference are investigated by re-deriving the results of the exact field calculations from a modified gradient/scattering framework, which explicitly takes into account the modification of the resonator field due to the particle.

ACKNOWLEDGMENTS

I am grateful to many people who have contributed directly and indirectly to his thesis. First and foremost is my doctoral advisor, Lev Deych. It is directly because of his emphasis on both mathematical rigor and intuitive understanding that this work has come to fruition. Much of the progress towards this thesis occurred at moments when, after my taking days or weeks to carefully derive and check mathematical results, Dr. Deych would pose a conceptual argument that called into question their validity. At the same time, he impressed upon me the importance of staying informed on current research and of properly articulating the substance and significance of one's own research. In the course of graduate school I felt a little bit of that excitement of discovering something new, and I am truly fortunate to have had a mentor who nurtured and encouraged that.

I am indebted to many of the professors and students in Physics department at Queens College, who were always willing to take valuable time assisting me when I needed help on a computation or finding an article. Professors Stephen Arnold of NYU-Polytech and Timothy Boyer of City College were also great sources of inspiration to this work and my love of science in general.

CONTENTS

LIST OF FIGURES

1. INTRODUCTION

This work began as a first-principles investigation of the electromagnetic interaction of a high-Q optical spherical microcavity a small dielectric scatterer. This is a topic for which there is already a great deal of theoretical and experimental literature on work on. Early research on spherical microcavities established the phenomenon of resonant splitting of the modes, which was attributed to particle-induced coupling of degenerate counter-propagating modes [1, 2, 3, 4, 5, 6]. This led to the suggestion of using this phenomenon as a method of detecting small particles via their characteristic frequency shift. Proof of principle was demonstrated, and more precise studies were carried out showing the effect of the particle on the width and spatial distribution of the mode. The theoretical framework of counter-propagating mode coupling appeared sufficient to explain all of these results, albeit with some modifications put in by hand to match experimental data [7]. At the same time, studies of coupled microcavities were being carried out based on the theory of multiple scattering by spheres [8, 9, 10, 11]. This is a computationally intensive field owing to the difficulty in calculating the addition coefficients that connect spherical optical modes scattered by arbitrarily placed cavities. There is a simple connection between small-particle scattering and coupling by multiple cavities: a subwavelength particle is essentially just a small sphere. This point of view allowed for a rigorous theory of particle-cavity coupling that was also analytically tractable since the scatterer can only support the lowest order modes [12, 13]. However, immediately the situation became more interesting, as our analytical equations revealed important qualitative differences to the backscattering theory. First there was the fact that the resonant "splitting" was in fact the creation of a new resonance, shifted from the original, with the original one left unmodified. Second, there was a distinction between the modification of modes with different polarizations: TE modes with one shifted peak, TM with two. Finally, the spatial distribution of the field differed from the circumferentially

uniform mode of the ideal resonator, and the standing wave modes of the modal coupling theory. This showed that our simple theory was important for more than rigor, as it led to conceptual differences in the understanding of the interaction.

In addition to providing rigorous mathematical and conceptual foundation for understanding interaction between WGM modes of spherical resonators and static particles, the developed theory turned out to be indispensable in describing optical forces exerted by WGMs on subwavelength particles. Optical forcing of small particles, usually associated with optical tweezer applications [14, 15], is of interest due to the possibility of optical cooling of macroscopic objects bound by optical traps [16, 17, 18, 7, 19, 20]. Additionally, interest in the long range motion of optically forced but unbound particles was ignited by a discovery from Steve Arnold and his co-workers of a WGM "carousel effect" [21]. It was demonstrated in their paper that a WGM was able to draw a particle suspended in liquid towards the resonator and set it into orbital motion. The circulatory motion was attributed to the circumferential force of the circulating angular momentum of the mode. However, rigorous evaluation of the optical force based on the developed theory of the resonator-particle interaction, revealed that the situation is more complicated than has been previously thought [22]. Instead of the expected exponential decay of the force in the evanescent region, we found a sharply peaked Lorenztian that was maximal a distance from the cavity walls. Moreover, the derived equations showed that the circumferential force has, in addition to a purely scattering component, proportional to the square of particle's polarizability, has an additional, linear in polarizability, contribution. The non-scattering part of the force was also non-conservative, counter to expectations. Using the heuristically defined 'photon number' to write the polarization energy in standard quantum form, we found that the force was generated by differentiating this energy but holding photon number constant. This was intriguing result, but one that I was still uncomfortable with. I had all the exact equations written on paper, I saw how to re-write them in a conceptually meaningful way, but I could not see

the connection between them. Furthermore, the point was trivial once it was understood, and was not of much use since one had to determine the self consistent field distribution in the first place. The first paper we published on this was again filled with cumbersome formulas which could not replace the appeal of existing heuristics. All the while, we had been pouring over classic textbooks to be sure of every step in the standard formulas for optical forces. Soon I realized that the constant photon number concept was in fact the distinction between the gradient over the extent of the particle, and the difference due an actual displacement of the particle and the re-adjustment of the field in the steady state. We termed this the "psuedo-gradient" [23]. We turned toward developing a theory to verify our optical forces, while I focused on elucidating the precise connection between the exact theory and the heuristics so that it could be presented and understood in a simple and more intuitive which wold also allow for expansion of our results to analytically intractable geometries such as toroidal WGM. While carousel effect has motivated the original work, it is not an easy experiment to use for verification of our findings. Therefore, we also considered the process of scattering of small particles by the field of spherical resonator, proposing that observation of this phenomenon can lead to a direct experimental verification of the proposed theory.

This led to an analysis of scattering of particles off the resonator, with a focus on inelastic effects. This provided a means to test the developed theory. Eventually, we realized how to derive these results in a more general matter that we believe should hold for other ring resonators.

2. Background

2.1 Vector Spherical Harmonics

Maxwell's equations in a linear medium are:

$$\nabla \cdot \mathbf{D} = \rho \qquad \nabla \times \mathbf{H} = \mathbf{J} + \frac{\partial \mathbf{D}}{\partial t} \tag{2.1}$$

$$\nabla \cdot \mathbf{B} = 0 \qquad \nabla \times \mathbf{E} + \frac{\partial \mathbf{B}}{\partial t} = 0 \tag{2.2}$$

where $\mathbf{D} = \epsilon \mathbf{E}$, $\mathbf{B} = \mu \mathbf{H}$, and ϵ and μ are the permittivity and permeability. In free space, $\epsilon = \epsilon_0$, $\mu = \mu_0$ and $\epsilon_0 \mu_0 = 1/c^2$ where $c = 2.9979 \times 10^8 m/s$ is the speed of light. We will assume that the medium is non-magnetic, $\mu = \mu_0$, loss free, isotropic and homogenous, ϵ real scalar, and source-free, $\rho, \mathbf{J} = 0$. We will also work in frequency domain where a vector $\mathbf{C}$ can be represented via Fourier transforms by the relation $\mathbf{C} = \int d\omega \ \tilde{\mathbf{C}} \ e^{-i\omega t}$. Given these constraints, and using the same symbol for time and frequency domain quantities, Maxwell's equation's become:

$$\nabla \cdot \mathbf{D} = 0 \qquad \nabla \times \mathbf{H} + i\omega \mathbf{D} = 0 \tag{2.3}$$

$$\nabla \cdot \mathbf{B} = 0 \qquad \nabla \times \mathbf{E} - i\omega \mathbf{B} = 0 \tag{2.4}$$

These equations can be de-coupled, and any of the four quantities obey the Helmholtz equation:

$$\nabla^2 \mathbf{C} + k^2 \mathbf{C} = 0 \tag{2.5}$$

where $k^2 = \mu_0 \epsilon \omega^2$. The Helmholtz operator is scalar, and thus acts on each vector component separately. Therefore, each Cartesian component of $\mathbf{C}$ is a solution to the scalar wave

equation:

$$\nabla^2\psi + k^2\psi = 0 \tag{2.6}$$

The solutions to Eq. 2.6 are $\psi_{l,m} = g_l(kr)Y_{l,m}(\theta,\phi)$, where $Y_{l,m}(\theta,\phi)$ is the spherical harmonic of order l, m and the radial function $g_l(kr)$ can be the spherical Bessel function $j_l(kr)$ or the spherical Nuemann function $n_l(kr)$. Usually, solutions inside of some bounded region employ spherical Bessel functions, while solutions in radiating regions employ the spherical Hankel functions $h_l = j_l + in_l$.

Taken on it's own, Eq. 2.5 has three independent solutions [24]. However, solutions to Maxwell equations must have the additional property of zero divergence and must be related to each other as $\nabla \times \mathbf{C}_1 = -ik\mathbf{C}_2$, $\nabla \times \mathbf{C}_2 = ik\mathbf{C}_1$. Following Jackson's derivation [25], note the vector identity:

$$\nabla^2(\mathbf{r}\cdot\mathbf{A}) = \mathbf{r}\cdot(\nabla^2\mathbf{A}) + 2\nabla\cdot\mathbf{A} \tag{2.7}$$

which shows that divergence free fields have a radial component which is a solution to Eq. 2.6, $\mathbf{r}\cdot\mathbf{C}_1 = \psi$. In terms of the other solution, this can be written: $k\mathbf{r}\cdot\mathbf{C}_1 = i^{-1}\mathbf{r}\cdot(\nabla\times\mathbf{C}_2) = i^{-1}(\mathbf{r}\times\nabla)\cdot\mathbf{C}_2$. The whole term to the left of $\mathbf{C}_2$ is an operator $\mathbf{L}$:

$$\mathbf{L} = \frac{1}{i}\mathbf{r}\times\nabla \tag{2.8}$$

which can be recognized as the quantum mechanical angular momentum operator, up to a factor of $\hbar$. In this context it cannot be interpreted as an "angular momentum" operator, but it is the generator of infinitesimal rotations. We see that, since $k\mathbf{r}\cdot\mathbf{C}_1 = \mathbf{L}\cdot\mathbf{C}_2$, that $\mathbf{L}\cdot\mathbf{C}_2$ is also a solution to Eq. 2.6. The properties of $\mathbf{L}$ are well known. The eigenfunctions of $\mathbf{L}\cdot\mathbf{L} = L^2$ are the spherical harmonics $Y_{lm}(\theta,\phi)$:

$$L^2Y_{lm}(\theta,\phi) = l(l+1)Y_{lm}(\theta,\phi) \tag{2.9}$$

It's Cartesian components $L_i = \hat{x}_i \cdot \mathbf{L}$, where $\hat{x}_i$, $i = 1, 2, 3$ are the Cartesian unit vectors, can be written in terms of the "raising" and "lowering" operators $L_x = (L_+ + L_-)/2$, $L_y = (L_+ - L_-)/2i$, where:

$$\begin{aligned} L_+ Y_{l,m} &= \sqrt{(l-m)(l+m+1)} Y_{l,m+1} \\ L_- Y_{l,m} &= \sqrt{(l+m)(l-m+1)} Y_{l,m-1} \end{aligned} \tag{2.10}$$

while the L_z component has the eigenvalue equation:

$$L_z Y_{l,m} = m Y_{l,m} \tag{2.11}$$

Since $\mathbf{L} \cdot \mathbf{C}_2$ is a solution to Eq. 2.6, $\mathbf{L} \cdot \mathbf{C}_2 \propto \psi_{l,m}$. This is satisfied for $\mathbf{C}_2 \propto \mathbf{L}\psi_{l,m} = g_l(kr)\mathbf{L}Y_{l,m}$, since then $\mathbf{L} \cdot \mathbf{C}_2 \propto g_l(kr)\mathbf{L} \cdot \mathbf{L}Y_{l,m} = g_l(kr)L^2 Y_{l,m} \propto \psi_{l,m}$. This also implies that the non-radial components of the curl of $\mathbf{C}_2$ satisfy Eq. 2.5. Writing $\nabla \times \mathbf{C}_2 \propto \nabla \times \mathbf{L}\psi$ and expanding the double curl $\nabla \times (\nabla \times \mathbf{a}) = \nabla(\nabla \cdot \mathbf{a}) - \nabla^2 \mathbf{a}$ gives $\mathbf{r} \times \nabla \times \mathbf{C}_2 = -\mathbf{r} \times \nabla(1 + rd/dr)\psi \propto (1 + rd/dr)g_l \mathbf{L}Y_{lm}$. Putting all this together, the conventional way to write these solutions is to first define:

$$\mathbf{X}_{l,m}(\theta, \phi) = \frac{1}{\sqrt{l(l+1)}} \mathbf{L} Y_{l,m}(\theta, \phi) \tag{2.12}$$

The "M polarized" solutions are then: $\mathbf{Z}_{l,m,M} = z_l(kr)\mathbf{X}_{l,m}(\theta, \phi)$, where z_l can denote either the spherical Bessel or spherical Hankel function. The solution $\mathbf{C}_2$ becomes

$$\mathbf{J}_{l,m,M} = j_l(kr)\mathbf{X}_{l,m}(\theta, \phi) \tag{2.13}$$

$$\mathbf{H}_{l,m,M} = h_l(kr)\mathbf{X}_{l,m}(\theta, \phi) \tag{2.14}$$

The "E polarized" solutions, $\mathbf{Z}_{l,m,E}$, are generated by applying the curl operator:

$$\mathbf{J}_{l,m,E} = \frac{-i}{k}\nabla \times [j_l(kr)\mathbf{X}_{l,m}(\theta,\phi)] \tag{2.15}$$

$$\mathbf{H}_{l,m,E} = \frac{-i}{k}\nabla \times [h_l(kr)\mathbf{X}_{l,m}(\theta,\phi)] \tag{2.16}$$

Their explicit forms are:

$$\mathbf{Z}_{l,m,M} = \frac{z_l}{\sqrt{l(l+1)}}\left(-\frac{mY_{l,m}}{\sin\theta}\hat{\theta} - i\frac{\partial Y_{l,m}}{\partial\theta}\hat{\phi}\right) \tag{2.17}$$

$$\begin{aligned}\mathbf{Z}_{l,m,E} &= \frac{z_l(kr)}{kr}\sqrt{l(l+1)}Y_{lm}\hat{r} \\ &\quad +[z_l(kr)kr]'\frac{1}{\sqrt{l(l+1)}}\left(\frac{Y_{l,m}}{\sin\theta}\hat{\theta} + i\frac{\partial Y_{l,m}}{\partial\theta}\hat{\phi}\right)\end{aligned} \tag{2.18}$$

and are known as Vector Spherical Harmonics (VSH). Note that the tangential component of $\mathbf{Z}_{l,m,E}$ obeys $\mathbf{Z}_{l,m,E} - \mathbf{Z}_{l,m,M} \cdot \hat{r} = -i[z_l(kr)kr]/(kr)\hat{r} \times \mathbf{X}_{l,m}$. Thus $\mathbf{Z}^*_{l,m,E} \cdot \mathbf{Z}_{l,m,M} = 0$. The orthogonality properties of the $\mathbf{Z}_{l,m,\sigma}$, $\sigma = E, M$ are determined by the orthogonality properties of $Y_{l,m}$ and $\mathbf{X}_{l,m}$, which obey:

$$\int d\Omega\ Y^*_{l',m'}(\theta,\phi)Y_{l,m}(\theta,\phi) = \delta_{l,l'}\delta_{m,m'}$$

$$\int d\Omega\ \mathbf{X}^*_{l',m'} \cdot \mathbf{X}_{l,m} = \delta_{l,l'}\delta_{m,m'} \tag{2.19}$$

$$\int d\Omega\ \mathbf{X}^*_{l',m'} \cdot (\mathbf{r} \times \mathbf{X}_{l,m}) = 0$$

This leads to:

$$\int dx\ d\Omega\ x^2\mathbf{Z}^*_{l',m',\sigma'} \cdot \mathbf{Z}_{l,m,\sigma} = \delta_{l,l'}\delta_{m,m'}\delta_{\sigma,\sigma'}\mathcal{N}_\sigma \tag{2.20}$$

where:

$$\mathcal{N}_\sigma = \int dx \begin{cases} x^2[j_l(x)]^2 & \text{if } \sigma = M \\ [j_l(x)]^2 + ([xj_l(x)]')^2 & \text{if } \sigma = E \end{cases} \tag{2.21}$$

The $\sigma = E$ case can be integrated by parts to give:

$$\mathcal{N}_E = \mathcal{N}_M + xj_l(x)\left(j_l(x) + xj_l(x)'\right) \tag{2.22}$$

2.1.1 Rotational and Translational Properties

The $\mathbf{Z}_{l,m,\sigma}$ are eigenmodes of generator of rotations, so they span a representation of the group of $3D$ rotations just like the scalar spherical harmonics $Y_{l,m}$. Consider two coordinate systems related by rotation about Euler angles α, β, γ, so that their position vectors $\mathbf{r}, \mathbf{r}'$ transform as $\mathbf{r}' = \mathbf{A}\mathbf{r}$, where:

$$\mathbf{A} = \begin{pmatrix} \cos\alpha\cos\beta\cos\gamma - \sin\alpha\sin\gamma & \sin\alpha\cos\beta\cos\gamma + \cos\alpha\sin\gamma & -\sin\beta\cos\gamma \\ -\cos\alpha\cos\beta\sin\gamma - \sin\alpha\cos\gamma & -\sin\alpha\cos\beta\sin\gamma + \cos\alpha\cos\gamma & \sin\beta\sin\gamma \\ \cos\alpha\sin\beta & \sin\alpha\sin\beta & \cos\beta \end{pmatrix} \tag{2.23}$$

The irreducible representation of rotation in the l, m basis is the Wigner D-matrix, $D^{(l)}_{m',m} = e^{-im'\alpha} d^{(l)}_{m',m}(\beta) e^{im\gamma}$, where:

$$\begin{aligned} d^{(s)}_{m,n} &= \sqrt{(s+m)!(s-m)!(s+n)!(s-n)!} \\ &\quad \times \sum_k (-1)^k \frac{(\cos\frac{\beta}{2})^{2s-2k+m-n} (\sin\frac{\beta}{2})^{2k-m+n}}{k!(s+m-k)!(s-n-k)!(n-m+k)!} \end{aligned} \tag{2.24}$$

The $\mathbf{Z}_{l,m,\sigma}$ fields can be represented in the primed system in terms of modes of the unprimed system:

$$\mathbf{Z}_{l,m,\sigma}(\theta', \phi') = \sum_{m'=-l}^{l} D^{(l)}_{m',m}(\alpha, \beta, \gamma) \mathbf{Z}_{l,m',\sigma}(\theta, \phi) \tag{2.25}$$

The infinitesimal form of the D functions can be expressed in terms of a rotation vector $\epsilon = \phi\hat{\mathbf{n}}$, where $\phi \ll 1$ is the rotation angle and $\hat{\mathbf{n}}$ the unit vector along the rotation axis [26]:

$$\begin{aligned} D^{(j)}_{m',m}(\epsilon) &= (1 - im\epsilon_z)\delta_{m',m} \\ &\quad -\frac{i\epsilon_x + \epsilon_y}{2}\sqrt{(j-m)(j+m+1)}\delta_{m',m+1} \\ &\quad -\frac{i\epsilon_x - \epsilon_y}{2}\sqrt{(j+m)(j-m+1)}\delta_{m',m+1} \end{aligned} \tag{2.26}$$

where ϵ_x , ϵ_y, and ϵ_z are the projections onto respective Cartesian axes.

Now consider two coordinate systems related by translation, $\mathbf{r}' = \mathbf{r} + \mathbf{d}$ where $\mathbf{d} = (d, \theta_t, \phi_t)$. The transformation of the fields is given by the addition theorem [27]:

$$\begin{aligned} \mathbf{Z}_{lmM}(\mathbf{r}') = \sum_{l'=1}^{\infty}\sum_{m'=-l'}^{l'} \Big[& \mathcal{A}^{l,m}_{l',m'}(i,k,\mathbf{d})\tilde{\mathbf{Z}}_{l'm'M}(\mathbf{r}) \\ & + \mathcal{B}^{l,m}_{l',m'}(i,k,\mathbf{d})(i\tilde{\mathbf{Z}}_{l'm'E}(\mathbf{r}))\Big] \end{aligned} \tag{2.27}$$

$$\begin{aligned} i\mathbf{Z}_{lmE}(\mathbf{r}') = \sum_{l'=1}^{\infty}\sum_{m'=-l'}^{l'} \Big[& \mathcal{A}^{l,m}_{l',m'}(i,k,\mathbf{d})(i\tilde{\mathbf{Z}}_{l'm'E}(\mathbf{r})) \\ & + \mathcal{B}^{l,m}_{l',m'}(i,k,\mathbf{d})\tilde{\mathbf{Z}}_{l'm'M}(\mathbf{r})\Big] \end{aligned} \tag{2.28}$$

where the tilde denotes $\mathbf{H}_{lm\sigma}$ for $|\mathbf{r}| > |\mathbf{d}|$ or $\mathbf{J}_{lm\sigma}$ for $|\mathbf{r}| < |\mathbf{d}|$. $\mathcal{A}^{l,m}_{l',m'}(i,k,\mathbf{d})$ and $\mathcal{B}^{l,m}_{l',m'}(i,k,\mathbf{d})$ are so called translation coefficients. The i index denotes the type of function dependance on the translation distance, d: $i = 0$ corresponds to j_l dependance while $i = \pm$ denotes $h^{(1,2)}_l = j_l \pm n_l$ function dependance. For $|\mathbf{r}| > |\mathbf{d}|$, $i = -$ and for $|\mathbf{r}| < |\mathbf{d}|$, $i = +$. The $i = -$ dependance is used in some of the symmetry relations of the coefficients. When the

translation vector undergoes inversion $\mathbf{d} \to -\mathbf{d}$, the translation coefficients obey [28]:

$$\mathcal{A}^{l,m}_{l',m'}(i,k,-\mathbf{d}) = (-1)^{l+L}\mathcal{A}^{l,m}_{l',m'}(i,k,\mathbf{d}) \tag{2.29}$$

$$\mathcal{B}^{l,m}_{l',m'}(i,k,-\mathbf{d}) = (-1)^{l+L}\mathcal{B}^{l,m}_{l',m'}(i,k,\mathbf{d}) \tag{2.30}$$

Interchange of modal indices $l', m' \to l, m$ for real k leads to, for $i = 0$:

$$\mathcal{A}^{l,m}_{l',m'}(0,k,\mathbf{d}) = (-1)^{l+L}\left[\mathcal{A}^{l',m'}_{l,m}(0,k,\mathbf{d})\right]^* \tag{2.31}$$

$$\mathcal{B}^{l,m}_{l',m'}(0,k,\mathbf{d}) = (-1)^{1+l+L}\left[\mathcal{B}^{l',m'}_{l,m}(0,k,\mathbf{d})\right]^* \tag{2.32}$$

while for $i = \pm$

$$\mathcal{A}^{l,m}_{l',m'}(\pm,k,\mathbf{d}) = (-1)^{l+L}\left[\mathcal{A}^{l',m'}_{l,m}(\mp,k,\mathbf{d})\right]^* \tag{2.33}$$

$$\mathcal{B}^{l,m}_{l',m'}(\pm,k,\mathbf{d}) = (-1)^{1+l+L}\left[\mathcal{A}^{l',m'}_{l,m}(\mp,k,\mathbf{d})\right]^* \tag{2.34}$$

2.1.2 Electromagnetic Quantities

A general monochromatic field can be expressed as a linear combination of VSH:

$$\mathbf{E} = E_0 e^{-i\omega t}\sum_{l=1}^{\infty}\sum_{m=-l}^{l}\sum_{\sigma=M,E}\left(C_{l,m,\sigma}\mathbf{H}_{l,m,\sigma}(\mathbf{r}) + P_{l,m,\sigma}\mathbf{J}_{l,m,\sigma}(\mathbf{r})\right) \tag{2.35}$$

while the magnetic field takes the form:

$$\begin{aligned}\mathbf{H} = -i\sqrt{\frac{\epsilon_0}{\mu_0}}E_0 e^{-i\omega t}\sum_{l=1}^{\infty}\sum_{m=-l}^{l} \quad & \left(C_{l,m,E}\mathbf{H}_{l,m,M}(\mathbf{r}) + C_{l,m,M}\mathbf{H}_{l,m,E}(\mathbf{r})\right. \\ & \left. + P_{l,m,E}\mathbf{J}_{l,m,M}(\mathbf{r}) + P_{l,m,M}\mathbf{J}_{l,m,E}(\mathbf{r})\right)\end{aligned} \tag{2.36}$$

That is, the magnetic field has the same expansion as the electric field but with polarization coefficients switched.

The type of radial function of the fields is determined by the boundary conditions at the origin and the radiation zone $kr \to \infty$. The spherical Bessel function $j_l(kr)$ is regular at the origin and can be used to describe the internal field, while the spherical Hankel function $h_l(kr)$ diverges and can only be used in the exterior region. In the radiation zone, $h_l(kr) \to (-i)^{l+1} e^{ikr}/kr$. In this region, the time dependant fields, $e^{-i\omega t}\mathbf{J}_{lm\sigma}$ and $e^{-i\omega t}\mathbf{H}_{lm\sigma}$ have respective phases $e^{-i\omega t}$ and $e^{-i(kr-\omega t)}$ times a constant factor. Thus $\mathbf{H}_{lm\sigma}$ fields describe traveling waves while the $\mathbf{J}_{lm\sigma}$ fields describe standing waves.

The energy density of the field is $\epsilon|\mathbf{E}|^2 + \mu_0|\mathbf{H}|^2$. It's integral over the volume element $r^2\ dr\ d\Omega$ gives the total energy. For a single mode with indices l, m, σ, this is:

$$E = \int r^2\ d\Omega\ \epsilon|\mathbf{E}|^2 + \mu_0|\mathbf{H}|^2 = \frac{\epsilon|E_0|^2}{4k^3} I_l$$

where:

$$I_l = \mathcal{N}_E + \mathcal{N}_M \tag{2.37}$$

The second term can be simplified using Eq. 2.22

$$I_l = 2\int dx\ x^2 |z_l(x)|^2\ +\ \ xz_l(x)\left(z_l(x) + xz_l'(x)\right)| \tag{2.38}$$

where prime denotes differentiation with respect to argument.

The power per unit area passing through the spherical surface at r is $\mathbf{S}\cdot\hat{r}$, where $\mathbf{S} = \mathbf{E}\times\mathbf{H}$.

The total power is thus:

$$P = \int r^2 \, d\Omega \, \mathbf{S} \cdot \hat{r}$$
$$= \frac{\epsilon |E_0|^2}{2k^2} c x^2 \, \mathcal{I}m \frac{z_l(x)^*}{x} \frac{d}{dx}[x z_l(x)] \tag{2.39}$$

The momentum density of the field is given by $\mathbf{S}/c^2$, and the angular momentum density as $\mathbf{r} \times \mathbf{S}/c^2$. The $\hat{z}$ component of angular momentum per unit length is:

$$M_z = \int r^2 \, d\Omega \, \hat{z} \cdot \left(\mathbf{r} \times \mathbf{S}/c^2 \right) = \frac{x^2}{ck} m |z_l(x)|^2 \tag{2.40}$$

The three quantities in Eq. 2.37 - Eq. 2.40 are generalized for a linear combination of modes, as in Eq. 2.35, by making the replacement $z_l \to c_{lm\sigma} h_l + p_{lm\sigma} j_l$ and summing over all modes. All components are independent of the polarization, which results because the electric and magnetic fields are always described by VSH wave functions with different polarizations.

In the far field region, the power becomes:

$$P = \frac{c\epsilon |E_0|^2}{2k^2} \begin{cases} 0 & \text{if } z_l = j_l \\ x^2 & \text{if } z_l = h_l \end{cases} \tag{2.41}$$

where use has been made of the fact that for $z_l = h_l$, the $\mathcal{I}m \; h_l^* d/dx[x h_l]$ term in Eq. 2.39 reduces to the Wronskian $W(j_l(x), n_l(x)) = 1/x^2$.

2.1.3 Resonances

An ideal lossless, homogenous, and isotropic spherical dielectric resonator can be modeled as a region of refractive index n_c up to radius R, surrounded by a medium of refractive index n_0. To find resonances, one expands the internal and scattered field of the sphere in terms of VSH, and the standard electrodynamic boundary conditions are imposed at $r = R$.

The internal and scattered fields are:

$$\mathbf{E}_{int} = E_0 \sum_{l,m,\sigma} p_{lm\sigma} \mathbf{J}_{lm\sigma} \tag{2.42}$$

$$\mathbf{E}_{scat} = E_0 \sum_{l,m,\sigma} c_{lm\sigma} \mathbf{H}_{lm\sigma} \tag{2.43}$$

with respective magnetic fields $\mathbf{H}_{int}$ and $\mathbf{H}_{scat}$. Setting $\hat{\mathbf{r}} \times \mathbf{E}_{int} - \mathbf{E}_{int} = 0$ and $\hat{\mathbf{r}} \times \mathbf{H}_{int} - \mathbf{H}_{int} = 0$ at the boundary, integrating over the solid angle and using the orthogonality properties, Eq. 2.19, leads to the following equation:

$$n_\sigma \frac{j_l'(nkR)}{j_l(nkR)} = \frac{h_l'(kR)}{h_l(kR)} \tag{2.44}$$

for every l, m, σ, where $n_\sigma = n/n_0$ for $\sigma = M$ and $n_\sigma = n_0/n$ for $\sigma = E$, $k = n_0\omega/c$, and $n = n_c/n_0$ is the relative refractive index of the cavity. This is a transcendental equation in x to be solved for each l and polarization. In general it will restrict the allowed values of k. For a given l, σ, there may be multiple k values which satisfy this equation, which are enumerated with the index s.

An incident field can be added, taking the form:

$$\mathbf{E}_{inc} = E_0 \sum_{l,m,\sigma} \eta_{lm\sigma} \mathbf{J}_{lm\sigma} \tag{2.45}$$

This incident field is added to the scattered field of the resonator. Application of the boundary conditions leads to the following expression for the scattered field coefficients:

$$c_{lm\sigma} = \alpha_{l\sigma} \eta_{lm\sigma} \tag{2.46}$$

where $\alpha_{l,\sigma}$ is the Mie scattering coefficient:

$$\alpha_{l,E} = -\frac{j_l(x)[x_i j_l(x_i)]' - n^2 j_l(x_i)[x j_l(x)]'}{h_l(x)[x_i j_l(x_i)]' - n^2 j_l(x_i)[x h_l(x)]'} = -\frac{N_{E,l}}{G_{E,l}}$$

$$\alpha_{l,M} = -\frac{j_l(x)[x_i j_l(x_i)]' - j_l(x_i)[x j_l(x)]'}{h_l(x)[x_i j_l(x_i)]' - j_l(x_i)[x h_l(x)]'} = -\frac{N_{M,l}}{G_{M,l}} \tag{2.47}$$

where $x_i = nkR$ and $x = n_0 kR$. The internal field is given by:

$$d_{lm\sigma} = \frac{in}{P_\sigma x}\frac{1}{N_{\sigma,l}} c_{lm\sigma} \tag{2.48}$$

where $P_E = n$ and $P_M = 1$. These scattering coefficients can be re-written as:

$$\alpha_{l\sigma} = -\frac{1}{1 + iG_{\sigma l}/N_{\sigma l}} \tag{2.49}$$

where:

$$\begin{aligned} G_{E,l} &= n_l(x)[x_i j_l(x_i)]' - n^2 j_l(x_i)[x n_l(x)]' \\ G_{M,l} &= n_l(x)[x_i j_l(x_i)]' - j_l(x_i)[x n_l(x)] \end{aligned} \tag{2.50}$$

It can be seen from Eq. 2.49 that for real x, the greatest magnitude of $\alpha_{l\sigma}$ is unity, which occurs when the imaginary part vanishes and the real part is -1. This means that the scattered field coefficients, Eq. 2.46, are perfectly out of phase with the incident field. The total field in the external region for a single mode source when $\alpha_{l\sigma} = -1$ is given by $\mathbf{E}_{ext} = \mathbf{E}_{inc} + \mathbf{E}_{scat} = \eta_{lm\sigma}\mathbf{J}_{lm\sigma} + c_{lm\sigma}\mathbf{H}_{lm\sigma} = \eta_{lm\sigma}(\mathbf{J}_{lm\sigma} - \mathbf{H}_{lm\sigma}) = i\eta_{lm\sigma}\mathbf{N}_{lm\sigma}$, where $\mathbf{N}_{lm\sigma}$ is defined analogously to $\mathbf{J}$ and $\mathbf{H}$ but with spherical Nuemann function (spherical Bessel of the second kind) dependance. As shown above, such a field corresponds to a standing wave, and by Eq. 2.39 there will be no net energy-momentum flux in the radial direction. Thus, in general, there is a real frequency for which the power flowing into the resonator from a given mode

equals the power flowing out. The more sharply peaked $\alpha_{l\sigma}$ is about it's maximum, the better the time-dependant field approximates a frequency eigenmode. The poles of $\alpha_{l\sigma}$ can be found by allowing the frequency to take on a complex value, $z = x + i\gamma$. The poles $z = x_l^{(0)} + i\gamma_l^{(0)}$ are simple [29] and the scattering coefficients can be expanded in a Laurent series about z_0. For very high Q modes, $\gamma_l^{(0)} \ll x_l^{(0)}$, and the Laurent series is valid on the real axis. Thus, as a function of real frequency, we have:

$$\alpha_{l,\sigma} \approx \frac{-i\gamma_l^{(0)}}{x - x_l^{(0)} + i\gamma_l^{(0)}} = \frac{-i\Gamma_l^{(0)}}{\omega - \omega_l^{(0)} + i\Gamma_l^{(0)}} \tag{2.51}$$

Since the resonances have small but non-zero width, they are termed "quasi-modes". This term can be justified by examining the field of the microsphere in the time domain. Consider a mode with internal field $\mathbf{E}(\mathbf{r},\omega) = p_{lm\sigma}\mathbf{J}_{lm\sigma}$, where $p_{lm\sigma} = \alpha_{l\sigma}$. In the time domain, this becomes $\mathbf{E}(\mathbf{r},t) = \int d\omega e^{-i\omega t}\mathbf{E}(\mathbf{r},\omega) \approx \mathbf{J}_{lm\sigma}(\mathbf{r},\omega_l^{(0)}) \int d\omega e^{-i\omega t}\alpha_{l\sigma} = -i\sqrt{2\pi}\Gamma_l^{(0)}\mathbf{E}(\mathbf{r},\omega_l^{(0)}) \exp(-i\omega_l^{(0)}t - \Gamma_l^{(0)}t)$.

Explicit formulae for resonance positions and widths can be found from asymptotic expansions for the Bessel and Hankel functions [30]. The leading terms of the resonant frequency are $x_l^{(0)} = \nu + 2.338(\nu/2)^{1/3} - P_\sigma/\sqrt{n^2-1} + O(\nu^{-1/3})$. Choosing for the incident field $\eta_{lm\sigma} = \delta_{l,L}\delta_{m,L}\delta_{\sigma,\sigma_0}$ corresponds to excitation of a fundamental WGM of order L with polarization σ_0.

A useful approximation for large l modes is to neglect quantities of order $1/l$. To order $l^{1/3}$, we can also use the eikonal $kR = x = O(l)$. In this case the recursion relations for the spherical Bessel functions reduce to:

$$\begin{aligned}(2l+1)x^{-1}z_l(x) = z_{l-1}(x) + z_{l+1}(x) &\rightarrow 2z_l(x) = z_{l-1}(x) + z_{l+1}(x) \\ (2l+1)z_l'(x) = lz_{l-1}(x) - (l+1)z_{l+1}(x) &\rightarrow 2z_l(x)' = z_{l-1}(x) - z_{l+1}(x)\end{aligned} \tag{2.52}$$

The ratio $|z_l(x)'/z_l(x)| = |(1-f)/(1+f)|$ where $f = z_{l+1}(x)/z_{l-1}(x)$, cannot exceed unity for $f > 0$. Since the order $l^{-2/3}$ correction to the resonant frequency is positive, x lies below the first zeros of z_{l-1}, z_l and z_{l+1} and consequently $f > 0$. Just outside the resonator, the argument of the radial function x_i is reduced due to the smaller refractive index, and is also below it's first zero. Therefore, the radial functions can be considered constant within a frequency range $x \pm \Delta x$ if $\Delta x \ll 1$. On the other hand $\alpha_{l,\sigma}$ can only be considered constant over the range $\Delta x \ll \gamma$. This introduces two separate frequency scales for the VSH functions and the scattering coefficients, and justifies pulling the VSH mode out of the Fourier transform. Applying the order of magnitude approximations $1/l \ll 1$, $x/l \approx 1$, $|z_l(x)'/z_l(x)| \approx 1$ to the VSH gives rise to simplified forms $\mathbf{Z}_{lmM} \rightarrow z_l(x)\mathbf{X}_{lm}(\theta,\phi)$, $\mathbf{Z}_{lmE} \rightarrow z_l(x)\left(\hat{r}Y_l^m(\theta,\phi) + \hat{r}\times\mathbf{X}_{lm}(\theta,\phi)\right)$. A mode in the general expansion over m,σ for a given $l \gg 1$ becomes in the time domain $\mathbf{E}_{lmM}(\mathbf{r},t) = (\int d\omega e^{-i\omega t} p_{lmM}(\omega) z_l(\omega nr/c))\mathbf{X}_{lm}(\theta,\phi)$ with the analogous expression for E modes. Here, frequency dispersion only couples time to the radial coordinate, leaving the angular part of the field identical to it's Fourier transform. If the separation of frequency scales is invoked, this becomes $\mathbf{E}_{lmM}(\mathbf{r},t) = \tilde{p}_{lmM}(t) z_l(xr/R)\mathbf{X}_{lm}(\theta,\phi)$.

We will only employ the $1/l \rightarrow 0$ approximation, labeling $l/x = \nu \approx n$. We will also use the ratio $(dn_l(x)/dx)/n_l(x) \approx \sqrt{\nu^2 - 1}$ [30].

The internal energy of the sphere is calculated by evaluating Eq. 2.37 between $r = 0$ and $r = R$:

$$E = \int r^2 \, d\Omega \, \epsilon|\mathbf{E}|^2 + \mu_0|\mathbf{H}|^2 = \frac{\epsilon|E_0|^2}{4k^3}\left(\mathcal{N}_E + \mathcal{N}_M\right)$$

The normalization integrals, $\mathcal{N}_\sigma$, are related by Eq. 2.21. If $j_l(kr)$ were to vanish at $r = R$, then $\mathcal{N}_E = \mathcal{N}_M$. Instead, the field at $r = R$ obeys the relation Eq. 2.44. Using the

approximation $Y_\nu/Y'_\nu \approx -\sqrt{\mu^2-1}$, where $\mu = l/kR$ and $\nu = l + 1/2$, $\mathcal{N}_M$ is:

$$\mathcal{N}_M = \frac{(nx_0)^2}{2} j_l(nx_0)^2 \left(n_\sigma^{-2}(\mu^2-1) + 1 - \frac{\nu^2}{(nx_0)^2} \right) \tag{2.53}$$

While the difference $\mathcal{N}_M - \mathcal{N}_E$ is:

$$\mathcal{N}_M - \mathcal{N}_E = \frac{(nx_0)}{2} j_l(nx_0)^2 \left(-2n_\sigma^{-2}\sqrt{\mu^2-1} + \frac{1}{nx_0} \right) \tag{2.54}$$

For $x_0 \gg 1$, the normalization factors are almost equal. A given mode excited by an ideal monochromatic source of frequency ω' has internal field in the frequency domain given by: $\mathbf{E} = a_{lm\sigma}\alpha_{l,\sigma}\delta(\omega - \omega')\mathbf{J}_{lm\sigma}$. If the resonant amplitude Eq. 2.51 is substituted for $\alpha_{l,\sigma}$ and and the Fourier transform is taken, the field is:

$$\mathbf{E}(t) = \int d\omega\ \mathbf{E}(\omega)\ e^{-i\omega t} = \frac{-i\Gamma_l^{(0)}\mathbf{J}_{lm\sigma}e^{-i\omega' t}}{(\omega - \omega') + i\Gamma_l^{(0)}} \tag{2.55}$$

Multiplying by the denominator of $\alpha_{l,\sigma}$ and recognizing that $d\mathbf{E}/dt = -i\int d\omega\ \omega\ \mathbf{E}$ yields a differential equation for $\mathbf{E}(t)$:

$$\frac{d\mathbf{E}(t)}{dt} = \left(-i\omega_l^{(0)} - \Gamma_l^{(0)} \right) \mathbf{E} + -\Gamma_l^{(0)}\mathbf{J}_{lm\sigma}e^{-i\omega' t} \tag{2.56}$$

The solution to Eq. 2.56 is:

$$\mathbf{E}(t) = ce^{-i\omega_l^{(0)}t - \Gamma_l^{(0)}t} + \frac{-\Gamma_l^{(0)}}{(\omega - \omega') + i\Gamma_l^{(0)}}\mathbf{J}_{lm\sigma}e^{-i\omega' t} \tag{2.57}$$

where c is a constant determined by initial conditions.

2.1.4 Multi-Sphere Mie Theory

A system of multiple spheres adds a new layer of complexity to the scattering problem since there is no longer a global spherical symmetry. Boundary conditions can be written for each sphere separately, but each sphere re-scatters the field of the other, and the two are expressed in different coordinate systems. The problem is solvable by use of the VSH addition theorem, Eq. 2.27, which allows a given mode, referenced to one coordinate system, to be expressed as a linear combination of modes referenced to a translated coordinate system. Take, for example, the case of two spheres which are centered at a coordinate systems that have position vectors $\mathbf{r}_i$, $i = 1, 2$ and related by translation $\mathbf{r}_i = \mathbf{r}_j + \mathbf{d}_{i,j}$. Incident, internal, and scattered fields of each sphere are expressed as a general VSH expansion Eq. 2.35. Now, the field scattered by one sphere adds to the total incident field of the other. Applying the index i to denote a given sphere, we have:

$$\mathbf{E}^{(i)}_{int} = E_0 \sum_{l,m,\sigma} p^{(i)}_{lm\sigma} \mathbf{J}_{lm\sigma}(\mathbf{r}_i) \tag{2.58}$$

$$\mathbf{E}^{(i)}_{scat} = E_0 \sum_{l,m,\sigma} c^{(i)}_{lm\sigma} \mathbf{H}_{lm\sigma}(\mathbf{r}_i) \tag{2.59}$$

$$\mathbf{E}^{(i)}_{inc} = E_0 \sum_{l,m,\sigma} \eta^{(i)}_{lm\sigma} \mathbf{J}_{lm\sigma}(\mathbf{r}_i) + \mathbf{E}^{(j)}_{scat}(\mathbf{r}_i) \tag{2.60}$$

where in the last equation j denotes the other sphere. The term $\mathbf{E}^{(j)}_{scat}(\mathbf{r}_i)$ represents the field scattered by sphere j expressed in the coordinate system centered at sphere i. It can be written by applying the addition theorem to the scattered field of each sphere Eq. 2.59:

$$\mathbf{E}^{(j)}_{scat}(\mathbf{r}_i) = \frac{1}{2} \sum_{l,l',m,m',\sigma,\sigma'} c^{(j)}_{lm\sigma} \mathcal{A}^{(\sigma,\sigma')}_{l,l',m,m'}(0, k, \mathbf{d}_{ij}) \mathbf{Z}_{l',m',\sigma'}(\mathbf{r}_i) \tag{2.61}$$

where $\mathcal{A}^{(E,E)}_{l,l',m,m'} = \mathcal{A}^{(M,M)}_{l,l',m,m'} = \mathcal{A}^{l',m'}_{l,m}$ and $\mathcal{A}^{(E,M)}_{l,l',m,m'} = \mathcal{A}^{(M,E)}_{l,l',m,m'} = \mathcal{B}^{l',m'}_{l,m}$. Applying the boundary conditions, we end up with the generalization of Eq. 2.46:

$$c^{(i)}_{lm\sigma} = \alpha_{l\sigma}\left\{\eta_{lm\sigma} + \sum_{l',m',\sigma'} c^{(j)}_{l',m',\sigma'}\mathcal{A}^{(\sigma,\sigma')}_{l,l',m,m'}(0,k,\mathbf{d}_{ij})\right\} \tag{2.62}$$

Evaluation of the translation coefficients are computationally intensive. Eq. 2.62 represents an infinite set of coupled linear equations. One simplification is to make use of the axial symmetry present in any two-sphere system. Since the orthogonality of m modes relies only on integration over the ϕ coordinate, the translation coefficients become diagonal in m when the spheres are situated along a common polar axis. Making use of symmetry relations Eq. 2.31 - Eq. 2.34, both the forward and reverse translation coefficients can be expressed as functions of the scalar translation distance d:

$$c^{(i)}_{lm\sigma} = \alpha_{l\sigma}\left\{\eta_{lm\sigma} + \sum_{l',\sigma'} c^{(j)}_{l',m',\sigma'}A^{(\sigma,\sigma')}_{l,l',m,m}(0,k,\pm d)\right\} \tag{2.63}$$

2.1.5 Hamiltonian for the Electromagnetic Field

As is well known from quantum optics, the Hamiltonian of a time harmonic electromagnetic mode of a closed cavity can be put in harmonic oscillator form. The Lagrangian density for the electromagnetic field is:

$$\mathfrak{L} = \frac{\epsilon_0}{2}\left[\left(\frac{\partial \mathbf{A}}{\partial t}\right)^2 - c^2\left(\nabla \times \mathbf{A}\right)\right] \tag{2.64}$$

where $\mathbf{A}$ is the vector potential in the Coulomb Gauge, $\nabla \cdot \mathbf{A} = 0$. Here the vector potential $\mathbf{A}$ plays the role of a generalized coordinate, while it's time and spatial derivatives are generalized velocities. In terms of electric and magnetic fields, Eq. 2.64 reads $\mathfrak{L} = \epsilon_0/2(\mathbf{E}^2 - c^2\mathbf{B}^2)$. The generalized momentum, $\mathbf{\Pi}$ corresponding to $\mathbf{A}$ is the partial derivative of the Lagrangian density with respect to $\dot{\mathbf{A}} = \partial\mathbf{A}/\partial t$, $\mathbf{\Pi} = -\epsilon_0\mathbf{E}$. The Hamiltonian density is

obtained by the Legendre transform $\mathfrak{H} = \mathbf{\Pi} \cdot \dot{\mathbf{A}} - \mathfrak{L}$. In terms of the fields:

$$\mathfrak{H} = \frac{\epsilon_0}{2}\mathbf{E}^2 + \frac{\mu_0}{2}\mathbf{H}^2 \tag{2.65}$$

If the field can be expanded in terms of frequency eigenmodes $\mathbf{A} = \sum \mathbf{A}_i$, where $\mathbf{A}_i = a_i e^{i\omega t}\mathbf{f}_i(\mathbf{r})$, then time derivatives can be taken explicitly. Assuming also that $\int |\mathbf{f}(\mathbf{r})|^2 d^3r = 1$, and $\int \mathbf{f}_i \cdot \mathbf{f}_j^* = 0$, The Hamiltonian becomes:

$$H = \int \mathfrak{H}\ d^3r = \sum_i H_i \tag{2.66}$$

where

$$H_i = 2\epsilon_0 \omega_i^2 |a_i|^2 \tag{2.67}$$

is the Hamiltonian for mode i. This permits definition of canonical variables $p_i = -\omega_i \epsilon_0 2\, \mathcal{R}e\, [a_i e^{-i\omega_i t}]$, $q_i = 2\, \mathcal{I}m\, [a_i e^{-i\omega_i t}]$, so that:

$$H = \sum_i \frac{p_i^2}{2\epsilon_0} + \frac{\epsilon_0 \omega_i^2}{2} q_i^2 \tag{2.68}$$

The Hamiltonian has the form of independent oscillators.

Since the high-Q modes of a microsphere act as quasi-eigenmodes which undergo damped harmonic motion, this procedure can be used. The $\mathbf{f}_i$ fields are simply the $\mathbf{Z}_{lm\sigma}$ functions with appropriate normalization over the interior of the resonator. For a spherical cavity there will be degenerate modes corresponding to modes with the same l, σ but different m values. Owing to the rotation properties of the VSH, one m mode becomes a linear combination of others upon coordinate rotation. The coefficients in the rotated system (the $D^{(l)}_{m,m'}$ functions) do not depend on l or σ, so the normalization of mode functions is unchanged.

The Hamiltonian Eq. 2.67 becomes:

$$H = 2\epsilon_0\omega^2 \sum_{m,l} |a_{m,l}|^2 \tag{2.69}$$

2.1.6 Review of Hamilton-Jacobi Theory

The Hamiltonian formulation of classical mechanics, in particular the Hamilton-Jacobi method, will be used widely in this paper. It is a framework which puts particle and electromagnetic field dynamics on an equal footing, serves as the natural platform for introducing non-conserving perturbations, provides a connection to geometric optics and will shed light on quantum-classical analogies.

Given n generalized coordinates q_i, $i = 1{-}n$, momenta p_i, and Hamiltonian $H(q_1...q_n, p_1...p_n)$, a transformation to new variables $Q_i = Q_i(q_1...q_n, p_1...p_n, t)$,$P_i = P_i(q_1...q_n, p_1...p_n, t)$ and "Hamiltonian" $K(Q_i...Q_n, P_i...P_n, t) = H + dF/dt$, where F is the generating function, is said to be *canonical* if it preserves the structure of the dynamical equations [31]:

$$\frac{dq_i}{dt} = \frac{\partial H}{\partial p_i} \;\; ; \;\; \frac{dp_i}{dt} = -\frac{\partial H}{\partial q_i} \tag{2.70}$$

That is, if the dynamics are described by Eq. 2.70 with $q_i \to Q_i$,$p_i \to P_i$,$H \to K$. The point of the Hamilton-Jacobi method is to solve the dynamics of a Hamiltonian system by finding a canonical transformation to coordinates and momenta that are all constants of motion. Obviously this condition is satisfied for $K = H + dF/dt = 0$. This can be achieved by a type-2 transformation, with generating function F_2 depending on 'old' coordinates q_i and 'new' momenta P_i, related via the equations $p_i = \partial F_2/\partial q_i$ and $Q_i = \partial S/\partial P_i$. This generating function, up to a constant, is equal to the indefinite action integral $S = \int dtL + constant$, where L is the Lagrangian. The condition for the vanishing of K is known as the Hamilton-

Jacobi equation:

$$H(q_1, ...q_n, \frac{\partial S}{\partial q_1}, ...\frac{\partial S}{\partial q_n}, t) + \frac{\partial S}{\partial t} = 0 \tag{2.71}$$

If the Hamiltonian is independent of time, $H = E$ =constant, Eq. 2.71 is separable with solution $S = W(q_i, P_i) - Et$. The function W satisfies the equation $H(q_i, \partial W/\partial q_i) = E$. By writing $W = S + Et = \int L + H \; dt$ and using $H = \sum_i p_i \dot{q}_i - L$ leads to:

$$W = \int \sum_i p_i dq_i \tag{2.72}$$

This integral, written in terms of the old canonical variables, is just a formal expression since the dynamics of the canonical variables has not been determined yet. It's usefulness comes when it can be explicitly expressed in terms of the old coordinates and new, constant momenta. If the Hamilton-Jacobi equation is separable, so that the old momenta $p_i = \partial S/\partial q_i$ can be expressed in terms of q_i and the separation constants, Eq. 2.72 can be integrated directly.

The integration is along the actual path of q_i, and W may be a multi-valued function of the q_i if the motion of the system is bounded. The whole path can be separated into smaller paths along which the integrand is single valued. Of particular interest are periodic systems, where the contributions along individual paths are equal. In this case, the indefinite integral for a one-dimensional system is a whole number times the integral over a single period, $W = nI$, where:

$$I = \frac{1}{2\pi} \oint p \; d_q \tag{2.73}$$

Now consider a one dimensional periodic system of period T with a conserved Hamiltonian $H = E$ which depends on some constant parameter λ. If λ begins to change with time, the system in general ceases to be conservative and periodic. However, if the change of λ is slow on the time scale of the unmodified system, that is if $Td\lambda/dt \ll \lambda$, lowest order corrections

to the motion can be calculated by averaging the variation of λ over the trajectory of the conserved system. The average energy will be:

$$\frac{d\bar{E}}{dt} = \frac{d\lambda}{dt}\frac{\partial\bar{H}}{\partial\lambda} \tag{2.74}$$

where the time average means:

$$\bar{f} = \frac{1}{T}\int f\ dt \tag{2.75}$$

and all quantities under the integral evaluated for constant λ. Using the fact that $T = \int_0^T dt = \oint dq/(\partial H/\partial p)$, one derives that:

$$\frac{d\bar{E}}{dt} = -\frac{d\lambda}{dt}\frac{\oint (\partial p/\partial\lambda)\ dq}{\oint (\partial p/\partial E)\ dq} \tag{2.76}$$

Rearranging this equation gives $d\bar{I}/dt = 0$, where I is the action Eq. 2.73. Due to the vanishing of it's average time derivative for small changes in λ, the action is known as an *adiabatic invariant* [32].

The period of the system is related to the partial derivative of I with respect to energy. This can be seen from:

$$2\pi\frac{\partial I}{\partial E} = \oint \frac{\partial p}{\partial E}\ dq = \oint \frac{dq}{\partial H/\partial p} = T \tag{2.77}$$

To consider formally the evolution of the system with a time dependant parameter λ, one defines so-called canonical or action-angle variables by using the action W as a the generating function and I (for a constant λ) as the new momentum. The equations of transformation are $p = \partial W(q, I; \lambda)/\partial q$ and $w = \partial W(q, I; \lambda)/\partial I$ where w is the new coordinate or angle variable. The action W is now time dependant due to λ, so the Hamiltonian in action-angle coordinates becomes:

$$K = E(I; \lambda) + \frac{\partial W}{\partial t} \tag{2.78}$$

$E(I;\lambda)$ is the energy of a constant λ orbit and is assumed to depend only on I. Since all time dependance is contained in λ, the time derivative is written: $\partial W/\partial t = (\partial W/\partial\lambda)_{q,I}\dot{\lambda}$. The canonical equations becomes:

$$\frac{dI}{dt} = -\frac{\partial K}{\partial w} = -\left(\frac{\partial \Lambda}{\partial w}\right)\dot{\lambda} \tag{2.79}$$

where $\Lambda = (\partial W/\partial\lambda)_{q,I}$. From inverting Eq. 2.77, the frequency ω is the derivative of the Hamiltonian with respect to I at constant λ. Now we have:

$$\frac{dw}{dt} = -\frac{\partial K}{\partial I} = \omega(I;\lambda) + \left(\frac{\partial \Lambda}{\partial I}\right)\dot{\lambda} \tag{2.80}$$

2.1.6.1 Special Cases

Consider a harmonic oscillator with Hamiltonian given by

$$H = \frac{p^2}{2m} + \frac{m\omega^2 q^2}{2} \tag{2.81}$$

After substituting $S = W - Et$, the Hamilton-Jacobi equation is written:

$$E = \frac{1}{2m}\left(\frac{\partial W}{\partial q}\right)^2 + \frac{1}{2}m\omega^2 q^2 \tag{2.82}$$

which gives:

$$\begin{aligned} W &= m\omega \int \sqrt{\frac{2E}{m\omega^2} - q^2}\; dq \\ &= \frac{m\omega}{2} q\sqrt{\frac{2E}{m\omega^2} - q^2} + \frac{E}{\omega}\arcsin q\sqrt{m\omega^2/2E} \end{aligned} \tag{2.83}$$

and:

$$q = \sqrt{\frac{2E}{m\omega^2}}\sin w \tag{2.84}$$

$$p = \sqrt{2Em}\cos w \tag{2.85}$$

Substituting these back into Eq. 2.83:

$$W = \int p\ dq = \frac{2E}{\omega}\int \cos^2 w dw \tag{2.86}$$

The adiabatic invariant is just the integral Eq. 2.86 evaluated over a full period, $I = E/\omega$. This quantity, up to proportionality, is the average number of quanta of the harmonic oscillator. We demand that I remain constant when $E \to E + \delta E$, $\omega \to \delta\omega$, as long as these variations fit the criteria of slowness under which Eq. 2.76 was derived. Thus, $\delta I = 0$ gives:

$$\frac{\delta E}{E} = \frac{\delta\omega}{\omega} \tag{2.87}$$

2.1.6.2 Scattering Orbit

The Hamiltonian for a particle in a central force potential is:

$$H = \frac{p_r^2}{2m} + \frac{M^2}{2mr^2} + U(r) \tag{2.88}$$

Where p_r is the conjugate momentum to the radial coordinate and $M = mr^2\dot{\phi}$ the angular momentum. The Hamilton-Jacobi equation reads:

$$E = \frac{1}{2m}\left(\frac{\partial W}{\partial r}\right)^2 + \frac{M^2}{2mr^2} + U(r) \tag{2.89}$$

The equation is separable with solution $W = W_r(r) + W_\phi(\phi)$, where

$$W_r = \int \sqrt{2m(E - U(r)) - M^2/r^2}\ dr \tag{2.90}$$

and:

$$W_\phi = M\phi \tag{2.91}$$

For a full orbit, ϕ changes by 2π and thus the adiabatic invariant for the ϕ variable is simply M. It's variation gives:

$$\frac{\delta\phi}{\phi} = -\frac{\delta M}{M} \tag{2.92}$$

Thus, if to the central force there is added a non-conservative ϕ component which changes M, the scattering angle will change proportionately. This expression is useful for evaluation of effects on scattering of a small non-central force, which would result in slow change of the angular momentum.

2.1.6.3 Non-Hamiltonian Forces

The theory of adiabatic invariants is only useful if the variation of the parameter λ is known explicitly, such as when it is a known function of time. For resistive functions and some non-central forces, it will be a function of the coordinates or momenta themselves, $d\lambda/dt = f(p,q)$. The adiabatic invariant will still be conserved, but the condition $\delta I = 0$, which was used above to determine the change in other quantities dependant on λ, is no longer useful since since $\delta\lambda$ depends on the trajectory of the system which it modifies. The first correction to λ can be obtained by integrating it's time derivative over a constant λ trajectory:

$$\delta\lambda^{(0)} = \frac{1}{T}\oint f(p,q)\ dt = \frac{1}{T}\oint \frac{f(p,q)}{\dot{q}}\ dq \tag{2.93}$$

In general further iterations will be necessary. There is one case however, where this first correction provides a definite result: when $f(p,q)/\dot{q}$ is proportional to p. Then $\delta\lambda^{(0)} \propto I$, and further iterations are unnecessary since the adiabatic invariant remains conserved.

Consider for example, homogenous decay such as that found in a harmonic oscillator with damping force $\dot{q}$:

$$\frac{d\bar{E}}{dt} = -2\Gamma E = -2\Gamma\omega I \tag{2.94}$$

Using $\partial E/\partial I = \omega$, this equation can be rearranged and integrated to give:

$$I(t) = I_0 \exp\{-2\Gamma t\} \tag{2.95}$$

where $I_0 = E/\omega$ is the adiabatic invariant evaluated over a period where λ is constant.

2.1.7 Optical Forces

The conservation of momentum for a system of fields and particles is given by [25, 33]:

$$\frac{d\rho}{dt} = \nabla \cdot \mathbf{T} - \frac{1}{c^2}\frac{\partial}{\partial t}\mathbf{E} \times \mathbf{H} \tag{2.96}$$

where ρ is the momentum density and

$$\mathbf{T} = \epsilon_0 \mathbf{EE} + \mu_0 \mathbf{HH} - \mathbf{I}\frac{1}{2}\left(\epsilon_0 E^2 + \mu_0 H^2\right) \tag{2.97}$$

$\mathbf{T}$ is the Maxwell stress tensor, expressed in dyadic notation in Eq. 2.97. $\mathbf{I}$ is the unit dyadic $\mathbf{I} = \hat{x}\hat{x} + \hat{y}\hat{y} + \hat{z}\hat{z}$ with $\hat{x}, \hat{y}, \hat{z}$ the Cartesian unit vectors. This equation can be integrated over a volume V to render the force on material particles inside. For any spherical surface, the integration can be performed explicitly in terms of VSH functions. For a field given by Eq. 2.35, the Cartesian components of the force are [34]:

$$\begin{aligned} F_1 = F_x + iF_y \;\; = \;\; & \frac{2\pi\epsilon_0|E_0|^2}{k^2}\sum_{l=1}^{\infty}\sum_{m=-l}^{l}\left\{\frac{[(l-m)(l+m+1)]^{1/2}}{l(l+1)}f_1\right. \\ & + \left[\frac{l(l+2)(l+m+1)(l+m+2)}{(l+1)^2(2l+1)(2l+3)}\right]^{1/2} f_2 \\ & \left. + \left[\frac{l(l+2)(l-m)(l-m+1)}{(l+1)^2(2l+1)(2l+3)}\right]^{1/2} f_3\right\} \end{aligned} \tag{2.98}$$

$$F_2 = F_z = -\mathcal{R}e\frac{4\pi\epsilon_0|E_0|^2}{k^2}\sum_{l=1}^{\infty}\sum_{m=-l}^{l}\left\{\frac{m}{l(l+1)}f_4 + \left[\frac{l(l+2)(l-m+1)(l+m+1)}{(l+1)^2(2l+1)(2l+3)}\right]^{1/2} f_5\right\} \quad (2.99)$$

where:

$$\begin{aligned}
f_1 &= \tilde{a}_{l,m}\tilde{b}^*_{l,m+1} + \tilde{b}_{l,m}\tilde{a}^*_{l,m+1} - \tilde{p}_{l,m}\tilde{q}^*_{l,m+1} - \tilde{q}_{l,m}\tilde{p}^*_{l,m+1} \\
f_2 &= \tilde{a}_{l,m}\tilde{a}^*_{l+1,m+1} + \tilde{b}_{l,m}\tilde{b}^*_{l+1,m+1} - \tilde{p}_{l,m}\tilde{p}^*_{l+1,m+1} - \tilde{q}_{l,m}\tilde{q}^*_{l+1,m+1} \\
f_3 &= \tilde{a}_{l+1,m}\tilde{a}^*_{l,m+1} + \tilde{b}_{l+1,m}\tilde{b}^*_{l,m+1} - \tilde{p}_{l+1,m}\tilde{p}^*_{l,m+1} - \tilde{q}_{l+1,m}\tilde{q}^*_{l+1,m+1} \\
f_4 &= \tilde{a}_{l,m}\tilde{b}^*_{l,m} - \tilde{p}_{l,m}\tilde{q}^*_{l,m} \\
f_5 &= \tilde{a}_{l,m}\tilde{a}^*_{l+1,m} + \tilde{b}_{l,m}\tilde{b}^*_{l+1,m} - \tilde{p}_{l,m}\tilde{p}^*_{l+1,m} - \tilde{q}_{l,m}\tilde{q}^*_{l+1,m}
\end{aligned} \quad (2.100)$$

Here $\tilde{a}_{l,m} = ic_{lmE} - i\frac{1}{2}p_{lmE}$, $\tilde{b}_{l,m} = c_{lmM} - \frac{1}{2}p_{lmM}$, $\tilde{p}_{l,m} = i\frac{1}{2}p_{lmE}$, $\tilde{q}_{l,m} = \frac{1}{2}p_{lmM}$.

2.1.8 Conservation of Energy

The conservation of energy for charge and current densities ρ and $\mathbf{J}$ is:

$$\frac{\partial u}{\partial t} + \nabla\cdot\mathbf{S} = -\mathbf{J}\cdot\mathbf{E} \quad (2.101)$$

where u is the energy density Eq. 2.65 and $\mathbf{S} = \mathbf{E}\times\mathbf{H}$ is the Poynting vector. For complex fields with harmonic time dependance, the real parts must be taken before calculating any quantity that involves a product of fields. For two quantities $A = (a+ib)e^{i\omega t}$, $B = (c+id)e^{i\omega t}$ $\mathcal{R}eA\cdot\mathcal{R}eB = ac\cos\omega t^2 + bd\sin\omega t^2 - (ad+bc)\cos\omega t\sin\omega t$. If this is now averaged over a period, we have $<\mathcal{R}eA\cdot\mathcal{R}eB>= (ad+bc)/2 = \mathcal{R}e[A\cdot B^*]/2$. The term proportional to $(ad+bc) = \mathcal{I}mA\cdot B^*$ has zero average. Therefore the real and imaginary parts of the product $A\cdot B^*$ represent, respectively, the components of $\mathcal{R}eA\cdot\mathcal{R}eB$ with non-zero and zero average. The zero average component can be written $-(ad+bc)\cos\omega t\sin\omega t =$

$(4\omega)^{-1}(ad+bc)d\cos 2\omega t/dt$. In Eq. 2.101, the source term $\mathbf{J}\cdot\mathbf{E}$ is equal to the total work done per unit volume, so $(1/2)\mathcal{R}e\mathbf{J}\cdot\mathbf{E}^*$ represents the average power loss, while $(4\omega)^{-1}\mathcal{I}m\mathbf{J}\cdot\mathbf{E}^*$ is the modulus of a quantity of energy that oscillates with time and does not lead to net power loss. Therefore, if Eq. 2.101 is treated as complex equation, the real and imaginary parts represent lost and stored energy. Defining complex Poynting vector $\mathbf{S} = \mathbf{E}\times\mathbf{H}^*/2$, average electric and magnetic energy densities $w_e = \epsilon|\mathbf{E}|^2/4$, $w_m = \mu_0|\mathbf{H}|^2/4$, the integral version of Eq. 2.101 becomes:

$$\frac{1}{2}\int_V \mathbf{J}^*\cdot\mathbf{E}\; dV + 2i\omega\int_V (w_e - w_m)\; dV + \oint_S \mathbf{S}\cdot d\mathbf{a} = 0 \tag{2.102}$$

3. Electromagnetic Scattering

We now consider the electromagnetic interaction of the spherical resonator with a small dipole scatterer. A small particle can be modeled as a sphere since it's shape should not be important in the dipole approximation. In this way, the dipole scattering problem becomes an application of the multi-sphere Mie theory framework. The radius and refractive index of the particle are denoted R_p and n_p, while those of the resonator are R and n.

As described in Sec. 2.1.4, the total electromagnetic field is expanded in terms of incident, scattered and internal fields of each sphere, defined in respective coordinate systems $\mathbf{r}_i$ $i = 1, 2$. Defining three regions of space, (I) the exterior region of both spheres, (II) inside the resonator and (III) inside the particle, the field is:

$$\mathbf{E} = \begin{cases} \mathbf{E}_{inc} + \mathbf{E}_{scat}^{(1)} + \mathbf{E}_{scat}^{(2)} & r_1 > R, r_2 > R_p \\ \mathbf{E}_{int}^{(1)} & r_1 < R \\ \mathbf{E}_{int}^{(2)} & r_2 < R_p \end{cases} \tag{3.1}$$

Application of the boundary conditions leads to the system of equations Eq. 2.62. The resonator has an incident field that would, in the absence of the particle, have excited a single fundamental WGM of either TM or TE polarization with a given angular number $l = L$, dimensionless vacuum frequency $x_L^{(0)}$ and width $\gamma_L^{(0)}$ found from a complex pole of the Mie coefficients. To mimic the experimental situation of excitation by a tapered fiber, we also assume that this incident field impinges only on the main sphere, so that $\mathbf{E}_{inc}^{(2)} = 0$. In the coordinate system with the polar axis perpendicular to the plane of the mode this field distribution is described by a single VSH with $|m| = L$:

$$\mathbf{E}_{inc} = \mathbf{Z}_{L,L,\sigma_0} \tag{3.2}$$

As discussed in Sec. 2.1.4, the axial symmetry of the system allows Eq. 2.62 to be diagonalized in m, m'. This requires the coordinate systems of the two spheres to be oriented such that a common polar axis passes through both spheres. The field distribution of the fundamental WGM Eq. 3.2 in this coordinate system cannot be described as a single VSH, but requires a linear combination of VSHs with all $-L \leq m \leq L$, as in Eq. 2.25. In the primed system, the location of the center of the particle is denoted $\mathbf{r}_p = (d, \theta_p, \phi_p)$. The transformation to the unprimed system can be obtained by rotating $X'Y'Z'$ by Euler angles $\alpha = \phi_p$, $\beta = \theta_p$, $\gamma = 0$. A mode of the XYZ system is expressed in the $X'Y'Z'$ using Eq. 2.25, while the incident field Eq. 3.2 is expressed in the XYZ system by using the reverse rotation:

$$\mathbf{E}_{inc} = \sum_{m=-L}^{L} D^{L}_{m,L}(0, -\theta_p, -\phi_p)\mathbf{Z}_{L,m,\sigma_0} \tag{3.3}$$

The dipole approximation for the particle means that $n_p k R_p \ll 1$. The asymptotic form of the scattering amplitude $\alpha_{l,\sigma}(\rho)$ in the limit $\rho \to 0$ is:

$$\alpha_{l,\sigma}(\rho) \approx -\delta_{\sigma,E}\left[1 + i\frac{(2l+1)!!(2l-1)!!}{(l+1)\rho^{2l+1}}\left(\frac{l n_2^2 + l + 1}{n_2^2 - 1}\right)\right]^{-1} \tag{3.4}$$

This decays fast with increasing l, and vanishes for M polarization. If only the $l = 1$ mode is retained the scattering coefficients become:

$$\alpha_{l,\sigma}(\rho) \approx \delta_{\sigma,E}\delta_{l,1}\frac{-i\alpha_0}{1-\alpha_0} \approx -i\alpha_0(1+\alpha_0) \tag{3.5}$$

where

$$\alpha_0 = \frac{2}{3}\left(\frac{n_p^2 - 1}{n_p^2 + 2}\right)(kR_p)^3 \tag{3.6}$$

This quantity is related to the polarizability of a small particle [35]:

$$\alpha_{dip} = 6\pi\epsilon_0\frac{\alpha_0}{k^3}(1 + i\alpha_0) \tag{3.7}$$

The dipole field is E polarized but interacts with modes of the resonator with either polarization. This arises because the addition theorem couples VSH fields with different polarizations.

After applying the dipole approximation, Eq. 3.5, to the system, the system of equations Eq. 2.62 can be decoupled. The coefficients are:

$$a^{(1)}_{l,m,\sigma} = \alpha^{(1)}_{l,\sigma} D^{L}_{m,L} \left(\delta_{l,L}\delta_{\sigma,\sigma_0} + \alpha^{(1)}_{L,\sigma_0} \mathcal{A}^{(E,\sigma_0)}_{L,m,1,m}(kd) \mathcal{A}^{(E,\sigma)}_{l,m,1,m}(kd) \frac{\alpha^{(2)}_1}{1-\alpha^{(2)}_1 \Theta} \right) \tag{3.8}$$

where

$$\Theta = \sum_{l=1}^{\infty} \sum_{\sigma=E,M} \alpha^{(1)}_{l,\sigma} \mathcal{A}^{(E,\sigma)}_{l,m,1,m}(kd) \mathcal{A}^{(E,\sigma)}_{1,m,l,m}(-kd) \tag{3.9}$$

Using the symmetry relations of the translation coefficients, Eq. 2.31 - Eq. 2.34, this becomes:

$$\Theta = \sum_{l=1}^{\infty} \sum_{\sigma=E,M} \alpha^{(1)}_{l,\sigma} \left| \mathcal{A}^{(E,\sigma)}_{l,m,1,m}(kd) \right|^2 \tag{3.10}$$

The $\mathcal{A}^{(E,\sigma)}_{l,m,1,m}(kd)$ coefficients are denoted $\mathcal{A}^{(E,\sigma)}_{l,m,1,m}(kd) = U_{L,m,\sigma}$:

$$\begin{aligned} \mathcal{A}^{(E,E)}_{l,m,1,m}(kd) &= U_{L,m,E}(kd) \qquad (3.11) \\ &= \sqrt{\frac{3}{2}} \left[\sqrt{\frac{(l+1)(l+|m|)}{(2l+1)(|m|+1)}} z^{(j)}_{l-1}(kd) + (-1)^m \sqrt{\frac{l(l+1-|m|)}{(2l+1)(1+|m|)}} z^{(j)}_{l+1}(kd) \right] \end{aligned}$$

$$\mathcal{A}^{(E,M)}_{l,m,1,m}(kd) = U_{L,m,M}(kd) = -i\frac{\sqrt{3}}{2} m \sqrt{2l+1} z^{(j)}_l(kd) \tag{3.12}$$

The expansion coefficient for the small sphere is:

$$a^{(2)}_{1,m,E} = \frac{D^{(L)}_{m,L} \alpha^{(2)}_1}{1-\alpha^{(2)}_1 \Theta} \tag{3.13}$$

If the $l = L$ resonance is well separated from other resonances so that in its vicinity no WGMs with $l \neq L$ have their own resonances, we can assume that the largest contribution to Θ

comes from the term which contains the resonant scattering amplitude $\alpha^{(1)}_{L,\sigma_0}$. Separating these terms out we define the reduced sum, Θ' as:

$$\Theta' = \{\Theta - \alpha^{(1)}_{L,\sigma_0}[U_{L,m,\sigma_0}]^2\} \tag{3.14}$$

Using these definitions, the expansion coefficients for the resonator are:

$$a^{(1)}_{l,m,\sigma} = D^L_{m,L}\left\{\begin{array}{ll} \dfrac{(1-\alpha^{(2)}_1\Theta')}{[\alpha_{L,\sigma_0}]^{-1}(1-\alpha^{(2)}_1\Theta') - \alpha^{(2)}_1[U_{L,m,\sigma_0}]^2} & l=L; |m|\leq 1 \quad (a) \\ \dfrac{\alpha^{(1)}_{l,\sigma}\alpha^{(2)}_1 U_{L,m,\sigma_0}U_{l,m,\sigma}}{[\alpha_{L,\sigma_0}]^{-1}(1-\alpha^{(2)}_1\Theta') - \alpha^{(2)}_1[U_{L,m,\sigma_0}]^2} & l\neq L; |m|\leq 1 \quad (b) \\ \delta_{l,L}\delta_{\sigma,\sigma_0}\alpha^{(1)}_{l,\sigma} & |m|>1 \quad (c) \end{array}\right\} \tag{3.15}$$

3.1 Internal Particle

For a particle situated inside of the resonator, the field distribution is modified so that the internal region of the resonator, region (II), includes the field scattered by the particle, while the exterior region, (I), contains only the scattered field of the resonator.

$$\mathbf{E} = \left\{\begin{array}{ll} \mathbf{E}_{inc} + \mathbf{E}^{(1)}_{scat} & r_1 > R \\ \mathbf{E}^{(1)}_{int} + \mathbf{E}^{(2)}_{scat} & r_1 < R \\ \mathbf{E}^{(2)}_{int} & r_2 < R_p \end{array}\right. \tag{3.16}$$

Since the internal region of the resonator contains propagating fields, the boundary conditions Eq. 2.46 do not apply. Rather, a different system of equations connects the scattered and internal field coefficients of each sphere:

$$c^{(1)}_{l,m,\sigma} = \tilde{\alpha}^{(1)}_{l,\sigma}\sum_{\nu,\sigma'}\left[a^{(2)}_{\nu,m,\sigma}\mathcal{A}^{(\sigma,\sigma')}_{l,m,\nu,m}\right] - \frac{in}{xG_{\sigma,l}}\eta^{(1)}_{l,m,\sigma} \tag{3.17}$$

$$a^{(2)}_{l,m,\sigma} = \alpha^{(2)}_l\sum_{\nu,\sigma'}(-1)^{l+\nu}\left[c^{(1)}_{\nu,m,\sigma}\mathcal{A}^{(\sigma,\sigma')}_{l,m,\nu,m}\right] \tag{3.18}$$

$$a_{l,m,\sigma}^{(1)} = \frac{i}{x}\frac{c_{l,m,\sigma}^{(1)}}{\tilde{N}_{\sigma,l}} - \frac{\lambda_{\sigma,l}}{\tilde{N}_{\sigma,l}}\eta_{l,m,\sigma}^{(1)} \tag{3.19}$$

$$\tag{3.20}$$

where we introduce standard ($\alpha_{l,\sigma}$) and modified ($\tilde{\alpha}_{l,\sigma}$) Mie parameters:

$$\tilde{\alpha}_{l,\sigma} = -\frac{\tilde{N}_{\sigma,l}}{G_{\sigma,l}} \tag{3.21}$$

with numerators defined as:

$$\tilde{N}_{E,l} = h_l(x)[x_i h_l(x_i)]' - n^2 h_l(x_i)[x h_l(x)]' \tag{3.22}$$

$$\tilde{N}_{M,l} = h_l(x)[x_i h_l(x_i)]' - h_l(x_i)[x h_l(x)]' \tag{3.23}$$

and denominators the same as Eq. 2.50. Additional quantities $\lambda_{\sigma,l}$ in Eq. 3.19 are:

$$\lambda_{E,l} = j_l(x)[x_i h_l(x_i)]' - n^2 h_l(x_i)[x j_l(x_i)]' \tag{3.24}$$

$$\lambda_{M,l} = j_l(x)[x_i h_l(x_i)]' - h_l(x_i)[x_i j_l(x_i)]' \tag{3.25}$$

The expansion coefficients can be presented by defining sums $\tilde{\Theta}$ and $\tilde{\Theta}'$ analogous to the external case:

$$\tilde{\Theta} = \sum_{l=1}^{\infty}\sum_{\sigma=E,M}\tilde{\alpha}_{l,\sigma}^{(1)}\left|\mathcal{A}_{l,m,1,m}^{(E,\sigma)}(kd)\right|^2 \tag{3.26}$$

$$\tilde{\Theta}' = \{\tilde{\Theta} - \tilde{\alpha}_{L,\sigma_0}^{(1)}[U_{L,m,\sigma_0}]^2\} \tag{3.27}$$

Whereby, the expansion coefficients for the main sphere become:

$$a^{(1)}_{l,m,\sigma} = D^L_{m,L}\left\{\begin{array}{ll} \dfrac{1}{\tilde{N}_{\sigma_0,L}}\dfrac{\left[\lambda_{\sigma_0,L}\alpha^{(2)}_1[U_{L,m,\sigma_0}]^2+\tilde{N}_{\sigma,L}\left(1-\alpha^{(2)}_1\tilde{\Theta}'\right)\right]}{[\tilde{\alpha}_{L,\sigma_0}]^{-1}(1-\alpha^{(2)}_1\tilde{\Theta}')-\alpha^{(2)}_1[U_{L,m,\sigma_0}]^2} & l=L;|m|\leq 1 \quad (a) \\ \dfrac{n}{x^2G_{\sigma,l}\tilde{N}_{\sigma_0,L}}\dfrac{\alpha^{(2)}_1U_{L,m,\sigma_0}U_{l,m,\sigma}}{[\tilde{\alpha}_{L,\sigma_0}]^{-1}(1-\alpha^{(2)}_1\tilde{\Theta}')-\alpha^{(2)}_1[U_{L,m,\sigma_0}]^2} & l\neq L;|m|\leq 1 \quad (b) \\ \delta_{l,L}\delta_{\sigma,\sigma_0}\alpha^{(1)}_{l,\sigma} & |m|>1 \quad (c) \end{array}\right\} \tag{3.28}$$

3.2 Resonances

Resonances are found by examining the behavior of the expansion coefficients in a frequency range close to the ideal Mie resonance with $l = L$. In the vicinity of a single sphere resonance Mie coefficients α_{L,σ^0} can be presented in the form of a complex Lorentzian, Eq. 2.51:

$$\alpha^{(1)}_{L,\sigma_0}(z) \approx \frac{-i\gamma^{(0)}_L}{z-x^{(0)}_L+i\gamma^{(0)}_L} \tag{3.29}$$

The modified Mie parameters $\tilde{\alpha}_{L,\sigma}$ can be presented in a similar form differing only by an overall factor. Since $\gamma^{(0)}_L$ is very small for WGMs, the Mie parameters are the fastest changing quantities in Eq. 3.15 and Eq. 3.28. Therefore, using Eq. 3.29, and calculating all other quantities at $x = x^{(0)}_L$, we can present the coefficients $a^{(1)}_{l,m,\sigma}$ in the Lorentzian form with new poles $z_{L,m} = x_{L,m} - i\gamma_{L,m}$. For externally positioned defects the poles are

$$z_{L,m} = x^{(0)}_L - i\gamma^{(0)}_L - i\gamma^{(0)}_L\frac{\alpha^{(2)}_1[U_{L,m,\sigma_0}]^2}{1-\alpha^{(2)}_1\Theta'} \tag{3.30}$$

whereas for internal defects one has:

$$z_{L,m} = x^{(0)}_L - i\gamma^{(0)}_L - i\gamma^{(0)}_L\frac{\alpha^{(2)}_1}{1-\alpha^{(2)}_1\tilde{\Theta}'}\left(\frac{\tilde{N}_{\sigma_0,L}}{N_{\sigma_0,L}}\right)[U_{L,m,\sigma_0}]^2 \tag{3.31}$$

Separation of the real and imaginary parts of the last terms in Eq. 3.30 and Eq. 3.31 gives the frequency shifts and broadenings induced by interaction with the defect.

There are different resonances $z_{L,m}$ for the different values of m. The number of these resonances is determined by the m dependence of U_{l,m,σ_0}. Both functions vanish for $|m| > 1$, giving the standard Mie resonance. $U_{l,m,E}$ can take $m = 0$ or $|m| = 1$, while $U_{l,m,M}$ vanishes for $m = 0$ and it's square is identical for $m = \pm 1$. Thus for $\sigma_0 = E$ modes there are two additional defect induced resonances, while for $\sigma_0 = M$ modes there is one. Combining this with the response at the single sphere frequency for $|m| > 1$ we see that instead of a simple doublet our theory predicts either two or three peaks based on the polarization of the incident mode.

Another qualitative feature of the resonance conditions Eq. 3.30 and Eq. 3.31 is that they do not contain the $D^L_{m,L}(-\gamma, -\beta, -\alpha)$, and are therefore independent of the the angular position of the defect. Thus a change in the angular position of a defect does not change the position or width of the resonance. However, the appearance of $D^L_{m,L}(-\gamma, -\beta, -\alpha)$ in the numerator of Eq. 3.15 results in a dependance of the amplitude of the resonance on the angular coordinates of the defect, which is due to the longitudinal and latitudinal phase oscillations of the excited mode. On the other hand, a change in the defect's radial distance from the resonator always leads to a change in the resonant frequency. The assumption that intensity oscillations correspond to resonant frequency shifts was taken in Ref. [36] as confirmation of the backscattering paradigm. In fact, it is seen here that the amplitude and frequency of a resonance can be altered independently.

The validity of the solutions presented relies on the convergence of the infinite sums appearing in the definition of Θ and $\tilde{\Theta}$, which is not trivial since spherical Hankel functions entering these sums increase with increasing polar number l. Considering the asymptotic forms of the spherical Hankel functions of the first kind $h^{(1)}_l(\rho)$ in the limit $l \to \infty$, ρ

fixed [37], we can show that the terms in these sums behave in the limit of large l as:

$$\lim_{l\to\infty}\left\{\begin{array}{c}\alpha^{(1)}_{\nu,\sigma}[U_{\nu,m,\sigma}]^2\\ \tilde{\alpha}^{(1)}_{\nu,\sigma}[U_{\nu,m,\sigma}]^2\end{array}\right\}=\frac{3}{2}i\left(1-\frac{m^2}{2}\right)\frac{1-n_1^2}{1+n_1^2}\frac{\nu^2}{(kd)^3}\left\{\begin{array}{c}(R_1/d)^{2\nu+1}\\ -n_1^{-3}(d/R_1)^{2\nu+1}\end{array}\right\} \tag{3.32}$$

Eq. 3.32 proves the required convergence, given that d is always less than R_1 for internal defects, and always greater than R_1 for external defects.

3.3 Field of the Two sphere system

To verify the new resonance positions, we look at the power radiated by the whole system. The total field at a position outside the spheres, expressed in the XYZ system is $\mathbf{E}=\mathbf{E}^{(1)}_{scat}+\mathbf{E}^{(2)}_{scat}$ with the resonator expansion coefficients given by Eq. 3.15. The particle coefficients are given by Eq. 3.13, and are expressed in XYZ via the addition theorem, Eq. 2.59. The total field becomes:

$$\mathbf{E}=\sum_{l,l',m,m',\sigma,\sigma'}\left(c^{(1)}_{lm\sigma}+c^{(2)}_{lm\sigma}A^{(\sigma,\sigma')}_{l,l',m,m'}(\mathbf{d}_{ij})\right)\mathbf{Z}_{l',m',\sigma'}(\mathbf{r}_i) \tag{3.33}$$

Each l,m,σ mode radiates power given by Eq. 2.39, and the total radiated power is:

$$P=\frac{c\epsilon_0|E_0|^2}{2k^2}\sum_{l,m,\sigma}|c^{(1)}_{lm\sigma}+c^{(2)}_{lm\sigma}A^{(\sigma,\sigma')}_{l,l',m,m'}(\mathbf{d}_{ij})|^2 \tag{3.34}$$

In order to illustrate the general results obtained and discuss their experimental implications we calculated various physical quantities for the particular case of the TM mode $L=39$ with $n=1.59$, which corresponds to experimental situation considered in Ref. [38]. We choose the external defect to have the same refractive index $n_p=1.59$ and radius $R_p/R=0.008$, while the internal defect is modeled as a vacuum cavity with $n_p=1$ and the same radius. Both are positioned in the plane of the fundamental mode, where the interaction strength is strongest. These calculations require truncation of two types of infinite sums: first, the Θ or $\tilde{\Theta}$, and

second, the overall summation of VSHs over mode number l, required for the evaluation of the field itself. By checking convergency of the sums we determined that a reasonable accuracy for all calculated quantities is obtained when both sums are truncated at $l_{max} = 60$. We begin by presenting dependence of frequency shifts and broadening of the defect-induced resonances versus defect position. For external defects functions appearing in Eq. 3.30 - 3.31, are monotonically decreasing with d, resulting in smaller shifts and broadening at larger distances. This reflects the weakening of the interaction as the external defect is removed from the evanescent field concentrated at the surface of the sphere. This behavior is demonstrated in Fig. 3.1, where we have plotted relative frequency shift and broadening vs. defect distance for the $|m| = 1$ induced resonance for both the TM and TE polarized modes. It is interesting to note that the scattering is stronger for TE polarized modes as evidenced by the frequency shift and broadening.

For internal defects, the internal field of the resonator is strongly non-monotonous with a sharp peak slightly away from the surface. This field also behaves differently for $m = 0$ and $m = \pm 1$ azimuthal components. As a result the distance dependence of the spectral characteristics of the internal defect system is more complex, as it can be different for different resonances and is also non-monotonic. These properties can also be illustrated by the radiative power spectrum of the sphere-defect system. The results of these calculations for TM excitation are shown in Fig. 3.2 for different defect distances d. One can see that for both defect configurations the $m = 0$ resonance is shifted further from $x_L^{(0)}$ and is weaker than the $m = \pm 1$ resonance, signifying a much stronger interaction between the defect and the sphere for the mode with $m = 0$ then for modes with $|m| = 1$. The $m = 0$ mode corresponds to the orientation of the dipole moment of the defect along the Z-axes of the coordinate system, while for $m = \pm 1$ modes this dipole moment lies in the XY plane. Therefore, the difference between these two cases reflects the dependence of the interaction strength between the electric field and the dipole upon the orientation of the latter. This is one of the main

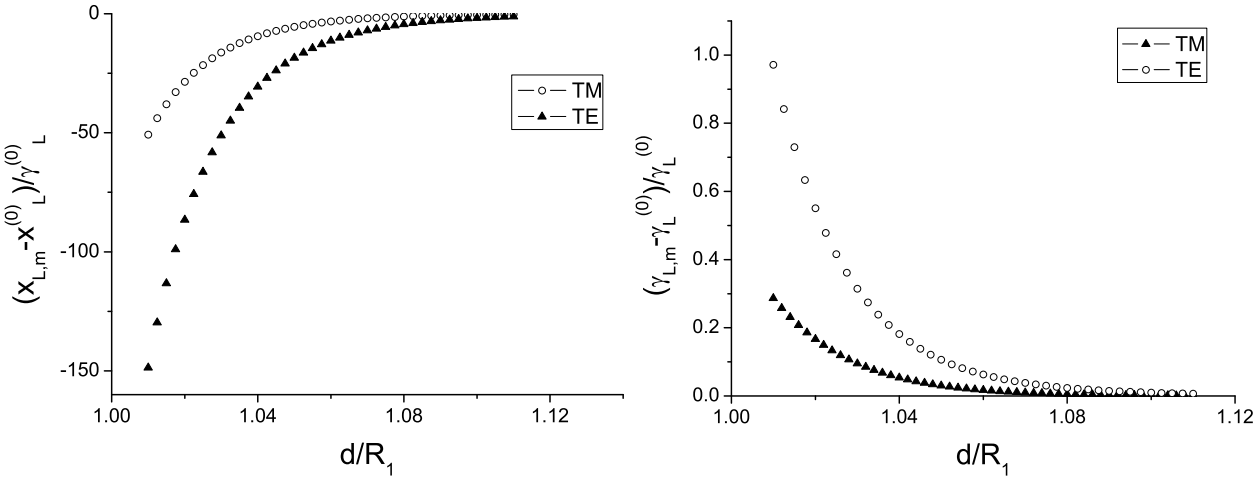

Figure 3.1: Frequency shift (left panel) and broadening (right panel) of the $|m| = 1$ resonance for an external defect with L=39 for both TM and TE polarization.

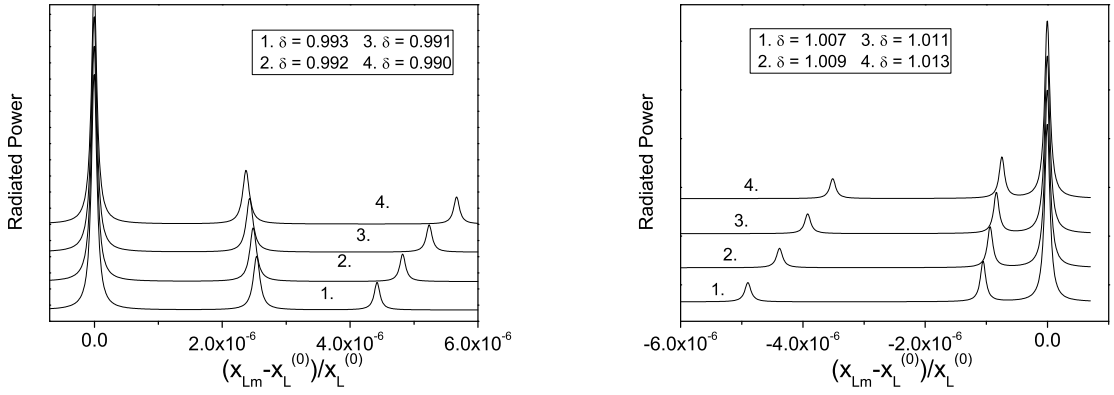

Figure 3.2: Radiated energy of the microsphere-defect system with varying distance $\delta = d/R$ for the internal (left panel) and external (right panel) defect cases.

factors overlooked by the traditional backscattering approach. This also explains why a TE polarized WGM, which has no radially outward component, gives rise to only the $|m| = 1$ resonance. The $m = 0$ peak is only found in TM polarized WGMs, and it's weakness makes it more difficult for experimental identification. We suggest, therefore, that the experimentally observed spectral doublets correspond to the original single-sphere resonance and the $m = \pm 1$ resonance introduced by the defect. The presence of the third peak can still be confirmed in an experiment with the controlled scattering of the type carried out in Ref. [36], but

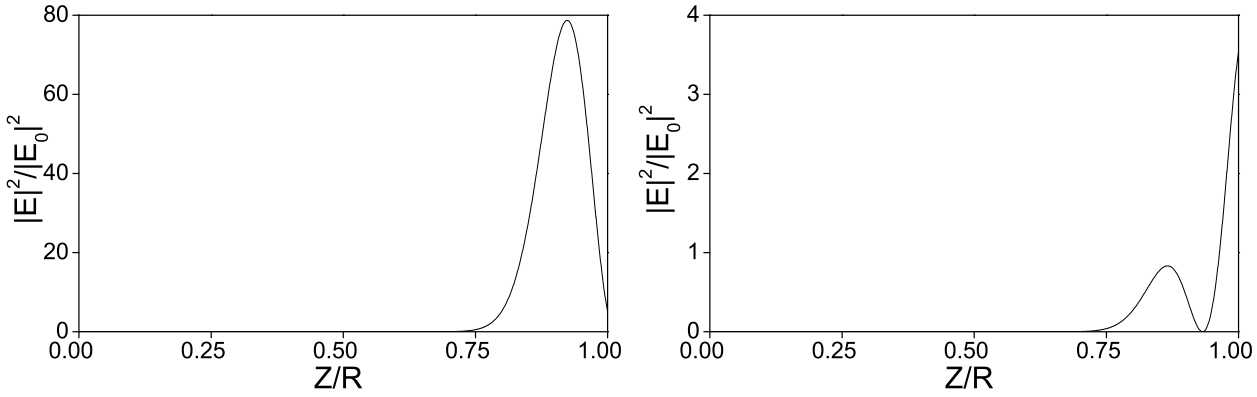

Figure 3.3: Field intensity in the radial direction of the unperturbed $m = 0$ (left panel) and $|m| = 1$ (right panel) modes.

covering a broader spectral range. This search might be complicated by the fact that the real microresonators are not ideal spheres so that their spectra contain many more spectral lines due to lifting of the degeneracy of the WGMs. In order to identify the additional defect related spectral feature in this situation one would have to purposefully study modifications of the spectrum caused by changing the position of the scatterer. The presented plots also demonstrate a significant difference between the internal and external defects. The most obvious of them is the difference in the sign of the frequency shift (red-shift for external defect and blue-shift for the external defect) caused by the difference in the relative refractive index of the defect for these two configurations. More fundamental is the difference in dependence of the magnitudes of the shifts upon the defect distance d. The monotonous decrease in the shift and broadening for both resonances of the external defect reflects the evanescent nature of the field outside of the resonator. In the case of the internal defect the $m = 0$ and $|m| = 1$ resonances demonstrate opposite behavior: as the defect is moved inward, away from the surface, the $|m| = 1$ peak moves closer to the single sphere resonance, while the $m = 0$ peak is pushed farther away. Since the magnitude of the shift is a measure of the strength of interaction, this behavior can be explained by examining the intensity of the field that interacts with the defect. Fig. 3.3 plots field intensity of the $m = 0$ mode and

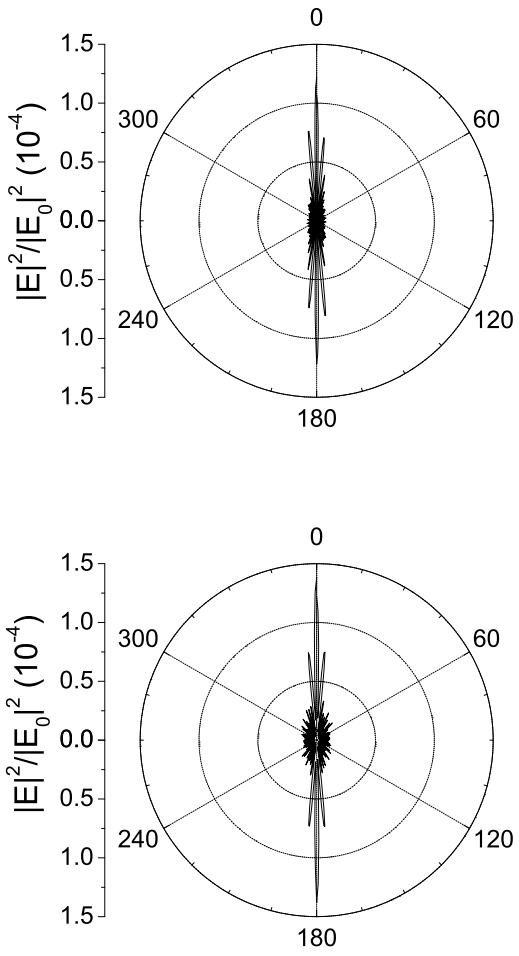

Figure 3.4: Directional plot of the radiated energy in the far-field for internal and external defect cases.

the sum of intensities of modes with $m = \pm 1$ as functions of the radial coordinate at the angular position of the defect's center. This figure shows that farther away from the surface the $|m| = 1$ field decreases and $m = 0$ field becomes stronger in agreement with behavior of the resonance frequency shifts. One can predict that moving the defect even further toward the sphere's center will result in non-monotonic behavior of the $m = 0$ peak, which will begin moving backward toward the unperturbed single-sphere resonance. Another important characteristic of the scattered field is the directional dependence of its intensity. It is more convenient to describe this dependence using the $X'Y'Z'$ coordinate system, whose

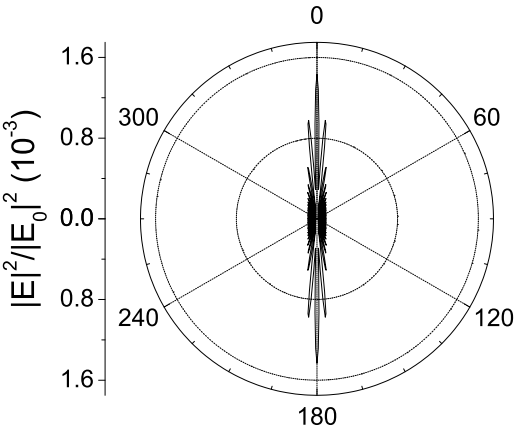

Figure 3.5: Scattered field of two $m = \pm 1$ modes excited in a single ideal sphere.

equatorial plane coincides with the plane of the initially excited FM. The dependence of the intensity upon azimuthal angle ϕ' of this coordinate system in its equatorial plane calculated for the $|m| = 1$ defect-induced resonance is shown in Fig. 3.4. In these simulations the defect was placed directly at the surface of the larger sphere for both internal and external configurations, and the intensity was calculated in the far field region. One can see that there is a drastic increase in the field intensity along the line that bisects the plane of the larger sphere and intersects the defect resulting in strong directionality of the scattering. A similar effect of defect-induced directionality of scattering in two-dimensional microdisk resonators was discussed recently in Ref. [39]. The narrowing of the emission cone occurs for both types of defects, but there are certain differences in the emission pattern for internal and external defects. The fundamental cause of this effect is similar for both configurations: the shift of the resonance frequency of $|m| = 1$ azimuthal components results in selective excitation of these particular modes at the respective frequencies. However, in the case of the external defect the structure of the scattering amplitudes for $m = \pm 1$ azimuthal components is similar to that of a single sphere. As a result, the scattered field pattern is also very close to that of an ideal sphere with two $m = \pm 1$ modes excited simultaneously. This assertion can be

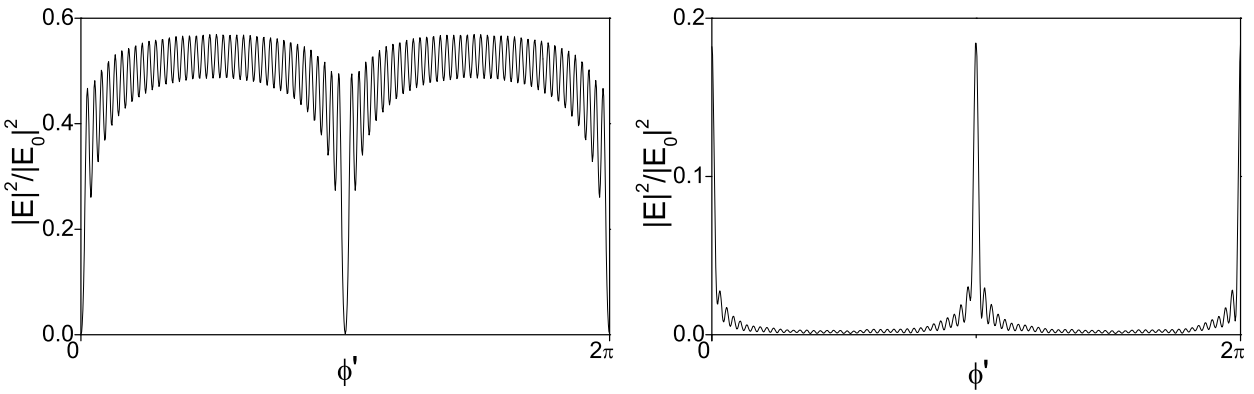

Figure 3.6: Variation of the surface field intensity with azimuthal coordinate in the primed system (ϕ') at the frequency of ideal Mie resonance (left panel) and the defect induced resonance (right panel).

verified by comparing Fig. 3.4 with Fig. 3.5, where the scattering intensity calculated for the latter situation is presented. In the case of the internal defect, in addition to the shift of the resonance frequencies, the defect changes the structure of the scattering amplitude (Eq. 3.28), which can be interpreted as a renormalization of the incident field expansion coefficients. As a consequence, the angular dependence of the scattered field in this case deviates stronger from the pattern associated with $m = \pm 1$ modes of the single sphere. The directional dependence of the intensity of the scattered field can be related to the spatial distribution of the internal field of the microsphere. To find this distribution one can use coefficients of the scattered field in combination with original coupled equations to calculate the expansion coefficients of the internal field. Fig. 3.6 plots the surface field intensity in the plane of the WGM for the external defect (the internal defect yields a very similar plot). At the frequency of the $|m| = 1$ defect-induced peak, the field profile demonstrates $2L$ oscillations and a drastic increase in intensity in the vicinity of the defect, which also manifests itself in the far field. At the frequency of the single-sphere resonance the situation is reversed: there are $2L$ oscillations which are phase shifted compared to the defect-induced resonance and are accompanied by a significant decrease in the field's intensity in the defect's proximity. Fig. 3.6 is again explained by the fact that the field at the defect-induced resonance is mainly

comprised of the m-components with $|m| = 1$. The field of these WGMs is characterized by $L - |m| + 1 = L$ oscillations for θ changing between $0, \pi$ giving their total number equal to $2L$. These modes are also characterized by the enhancement of the field in the vicinity of $\theta = 0$, which explains a drastic rise in the intensity around the location of the defect. The field distribution at the single sphere resonance can be understood by noting that this field is comprised of modes with $|m| > 1$, which when added to the remaining $|m| \leq 1$ components, would have produced a flat distribution of the intensity. Therefore, removal of these components obviously results in the decrease of the field around the defect and phase shifted oscillations elsewhere.

3.4 Optical Forces

With the full field of the resonator-particle system expressed in VSH, the force on the particle is obtained by using the Maxwell stress tensor. However, so far we have been expressing the field in a coordinate system centered at the resonator. To employ the Maxwell stress tensor, we must integrate over a surface enclosing the particle, so that the expansion coefficients in Eq. 3.15 are expressed in the system centered on the particle. Expression of the field in the system centered at the resonator requires only the translation coefficients where one index $l = 1$. In translating to the system centered at the particle, the expansion coefficients will be a sum over all coefficients with one $l = L$. There is no general expression for these coefficients, even if $L \gg 1$, so the field is much easier expressed in the resonator system. However, if both sphere and resonator are enclosed by the surface, the translation coefficients $U_{l,m\sigma}$ have bessel function dependance, and are negligible compared to radial functions with Hankel function dependance. Therefore, the total force on the system is approximately zero and Newton's third law holds. Thus, we can calculate the force on the

particle from the negative of the force on the resonator.

$$\mathbf{F} = -f_0 \mathcal{A} \left\{ \hat{r} + \frac{g}{y_0^2 + 1} \left(\left[(y_0 - y) + p(1 + y y_0) \right] \hat{\phi} + \bar{\theta} \left[(1 + y y_0) + p(y_0 - y) \right] \hat{\theta} \right) \right\} \tag{3.35}$$

where

$$f_0 = \frac{\mathcal{R}e\ [\alpha] |E_0|^2}{12\pi} \left(\frac{\Gamma_0}{\Gamma_p} \right)^2 \frac{k U_{L,1,\sigma_0}}{\sqrt{\pi L}} \left(U_{L-1,1,\sigma_0} - U_{L+1,1,\sigma_0} \right) \tag{3.36}$$

$$\mathcal{A} = \frac{e^{-L\bar{\theta}^2}}{y^2 + 1} \tag{3.37}$$

$\hat{r}$, $\hat{\theta}$ and $\hat{\phi}$ are the spherical coordinate unit vectors referred to the unprimed system, r_p is the translation distance, and $y = (\omega - \omega_p)/\Gamma_p$, where ω_p and Γ_p are the particle induced resonances corresponding to $m = \pm 1$. $\bar{\theta} = \theta - \pi/2$, $y_0 = (\omega - \omega_L^{(0)})/\Gamma_L^{(0)}$. Expression for parameter g depends on the polarization of the initial WGM of the resonator. If this mode is of magnetic type, we have

$$g_M = 2 \frac{\Gamma_p}{\Gamma_L^{(0)}} \frac{U_{L-1,1,M} + U_{L+1,1,M}}{U_{L-1,1,M} - U_{L+1,1,M}} \tag{3.38}$$

while for the electric modes, the contribution of the additional resonance with $m = 0$ modifies this expression to

$$g_E = \frac{\Gamma_p}{\Gamma_L^{(0)}} \frac{(U_{L-1,1,E} + U_{L+1,1,E})(1 + \frac{\Delta}{\Delta_E}) + \frac{\Delta}{\Delta_E} \frac{U_{L,0,E}}{U_{L,1,E}} (U_{L-1,0,E} + U_{L+1,0,E})}{U_{L-1,1,E} - U_{L+1,1,E}} \tag{3.39}$$

where $\Delta = \omega - \omega_L^{(0)}$ and

$$\Delta_E = \omega - \Gamma_L^{(0)} \frac{\mathcal{R}e\ \alpha [U_{L,1,E}]^2}{6\pi\epsilon_0}$$

Fig. 3.7 present the color plot of the forces for an initial WGM of electric type. One can see that all forces have Lorentzian form with a maximum at $y = 0$. The radial force is purely attractive, while the azimuthal force tends to push the particle in the $+\hat{\phi}$ direction.

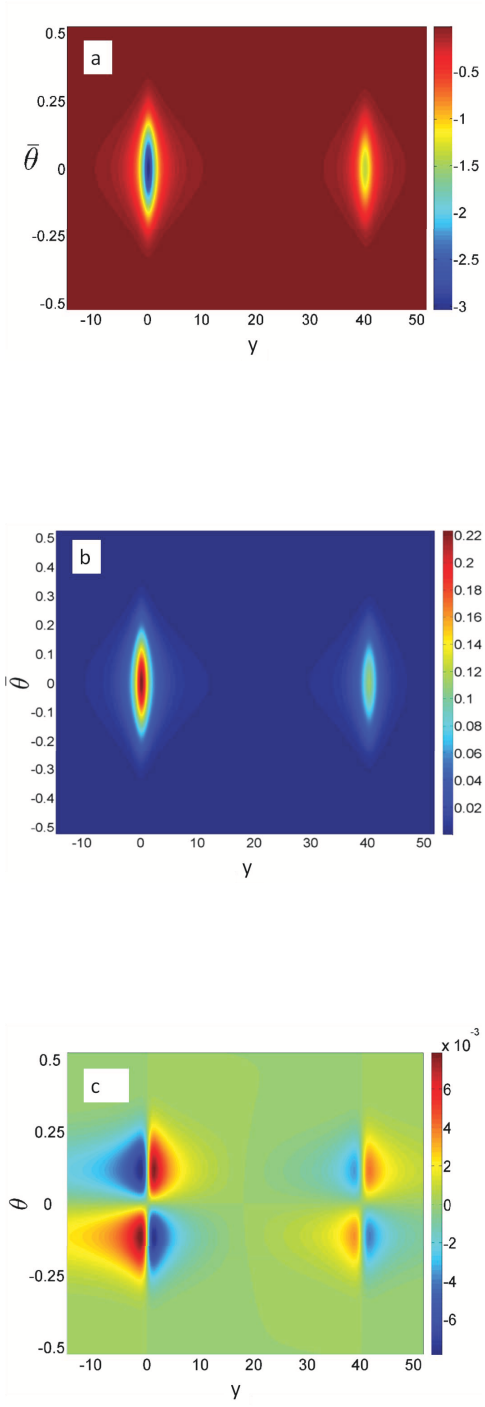

Figure 3.7: Vector components of the optical force in units of $\epsilon_0|E_0|^2/k^2$: F_r (a), F_ϕ (b), F_θ (c), for $L = 39$, E type mode, $R_p/R = 0.01$, $n = 1.59$, $\Gamma_L^{(0)}/\delta\omega = 100$.

Using the approximations described above for the limit $1/l \to 0$, we have

$$\frac{d\delta\omega}{dr_p} \approx -2\delta\omega k((L/x)^2 - 1)^{1/2} = -\frac{2L}{\rho r_p}\delta\omega$$

and the forces can be written:

$$F_r = -N\mathcal{A}\frac{d\delta\omega}{dr_p} \tag{3.40}$$

$$F_\theta = F_r\frac{\rho}{\bar{\Gamma}}\frac{\bar{\theta}}{y_0^2+1}(1 + yy_0 + p(y_0 - y)) \tag{3.41}$$

$$F_\phi = F_r\frac{\rho}{\bar{\Gamma}}\frac{1}{y_0^2+1}(y_0 - y + p(1 + yy_0)) \tag{3.42}$$

where $N = \epsilon_0|E_0|^2/2\sqrt{\pi L}\Gamma_L^{(0)}k^3$ and $\bar{\Gamma} = \Gamma_0/\Gamma_p$. The detuning y can be expanded about zero, $y = (r_p - r_0)y'$, where r_0 is the position where $\delta\omega = \omega - \omega_L^{(0)}$, and $y' = dy/dr_p = -(1 + yp)\delta\omega'/\Gamma_p$. The factor $(y^2+1)^{-1}$ becomes a Lorentzian in $r_p - r_0$ with effective width $1/y'$.

3.5 Optomechanical Trajectories

It is convenient to analyze particle dynamics by introducing dimensionless time $\tau = t/T$ and angular momentum $\zeta = M_P r_P^2\dot{\phi}\cos\bar{\theta}/\Lambda$, where $T = \sqrt{M_P r_0/f_0}$ and $\Lambda = \sqrt{M_P r_0^3 f_0}$. The de-tuning y, linearized about zero, can be used as a dimensionless radial coordinate of the particle, with the spatial width of the force characterized by dimensionless parameter $b = (y'(r_0)r_0)^{-1}$. The equations of motion in dimensionless form are:

$$\frac{d^2y}{d\tau^2} = \frac{1+yb}{b}\left(\frac{d\bar{\theta}}{d\tau}\right)^2 + \frac{\zeta^2}{b(1+yb)^3} + \frac{F_r}{bf_0} \tag{3.43}$$

$$\frac{d\zeta}{d\tau} = \zeta\left(\frac{d\bar{\theta}}{d\tau}\right)\tan\bar{\theta} + (1+yb)\frac{F_\phi}{f_0} \tag{3.44}$$

$$\frac{d^2\bar{\theta}}{d\tau^2} = \frac{-2b}{1+yb}\left(\frac{dy}{d\tau}\right)\left(\frac{d\bar{\theta}}{d\tau}\right) - \frac{\zeta^2\tan\bar{\theta}}{(1+yb)^4} + \frac{1}{(1+b)}\frac{F_\theta}{f_0} \tag{3.45}$$

where the terms proportional to ζ^2 are of usual kinematic origin, and $\zeta = (1+yb)^{-1}d\phi_p/d\tau \approx d\phi_p/d\tau$ is simply the angular velocity of the particle. To the first order in $\bar{\theta}$ and it's time derivatives the equations of motion for the particle take the form of

$$\frac{d^2y}{d\tau^2} = \frac{\zeta^2}{b(1+yb)^3} - \frac{1}{b(y^2+1)} \tag{3.46}$$

$$\frac{d\zeta}{d\tau} = \frac{\kappa g_\phi}{y^2+1} \tag{3.47}$$

$$\frac{d^2\bar{\theta}}{d\tau^2} = -\left(\zeta^2 + \frac{\kappa g_\theta y}{y^2+1}\right)\bar{\theta} \tag{3.48}$$

where $\kappa = \Gamma_L^{(0)}/\delta\omega$. Time and orbital momentum scales T and Λ correspond to the period and angular momentum for the circular orbit of radius r_0 in the $\bar{\theta} = 0$ plane in the absence of the azimuthal component of the optical force. The change in ζ over this time scale ($\Delta\tau = 1$) is $d\zeta/d\tau \approx \kappa g_\phi < 1$, which shows that the increase of angular momentum is slow over the orbital time scale. In this case the radial motion, described by Eq. 3.46, occurs in an effective slowly changing potential characterized by a stable equilibrium $y_0 = -\sqrt{\zeta^{-2}-1}$, which exists for $\zeta < 1$. However, if the angular velocity is too small the particle crashes on the surface of the resonator. Taking these two limitations into account one obtains that the radial motion of the particle can be trapped by the resonator if $\zeta_{min} < \zeta < 1$, where $\zeta_{min} = [((r_0 - R)/(br_0))^2 + 1]^{-1/2}$. In this case the radial motion can be approximately described as harmonic oscillations with adiabatically time-dependent frequency $\Omega_r = \zeta^2(-2y_0/b)^{1/2} > 1$.

When the particle deviates from the $\bar{\theta} = 0$ plane, second order terms in the $\bar{\theta}$ coordinate (neglected in Eq. 3.46-Eq. 3.48) arising from the factor $e^{-L\bar{\theta}^2}$ in the force in Eq. 3.37 can play a role since $L \gg 1$. For constant y, Eq. 3.48 describes harmonic oscillations about $\bar{\theta} = 0$ with frequency $\Omega_\theta \approx |\zeta| \ll \Omega_r$. Therefore, the effect of the polar dynamics on the radial coordinate can be described by replacing the expression for the equilibrium with $y_0 \to -\sqrt{y_0^2 - L\bar{\theta}^2/\zeta^2}$. This point oscillates with $\bar{\theta}$ over the time scale $\tau_\theta = 2\pi/\Omega_\theta$ while increasing overall due to the increase in ζ. This qualitative analysis is confirmed by a direct

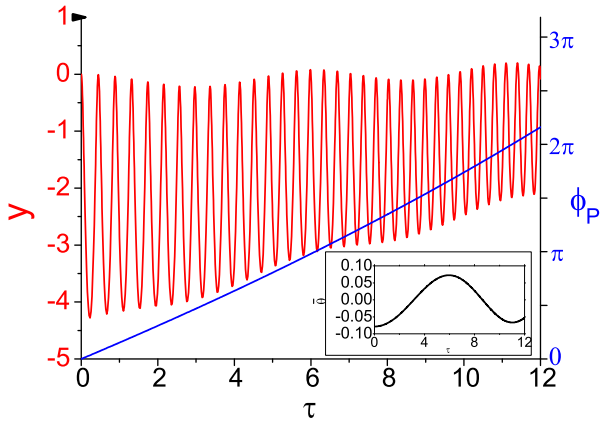

Figure 3.8: Time-dependence of particle's coordinates. The rapidly oscillating curve represents the radial coordinate, the monotones line in the main figure shows the azimuthal coordinate, and the insert shows the polar coordinate

numerical integration of Eq. 3.46 - Eq. 3.48 The analysis provided above is possible because of clear separation of time scales between orbital, polar and radial degrees of freedom with the latter being the fastest. Therefore, radial frequency Ω_r sets up limits of applicability of the unresolved side band approximation, which can now be formulated as $\Omega_r \ll T\omega_0/Q$. In terms of external parameters this inequality can be rewritten in the form of the lower limit on the mass of the particle: $M_P \gg (PQ)/(r_0^2 b^2 \omega^3)$. For instance, if $R_p = 100\ nm$, $R = 50\ \mu m$, $P = 50\mu W$, $\omega = 3 \times 10^{14} Hz$, which are typical values for experiments of this kind [21, 40] we obtain that quasi-static approximation for the field is valid for particles with $M_P \gg 10^{-16} g$. Minimum value of the orbital momentum allowing for the particle to orbit the resonator in this case is $\zeta_{min} \approx 0.12$. A particle with $M_P = 10^{-13}\ g$, similar to those used in Ref. [21], will be trapped by the radial quasi-potential if its linear velocity v is in the range $10\ cm/s < v < 100\ cm/s$. Numerical simulations of the particle's trajectories show that if the initial velocity of the particle is close enough to its minimum value, the particle will undergo at least one complete revolution before its tangential velocity reaches the upper critical value. To estimate feasibility of experimental observation of the orbital motion of particles in vacuum, one has to consider effects due to residual low-density gaseous

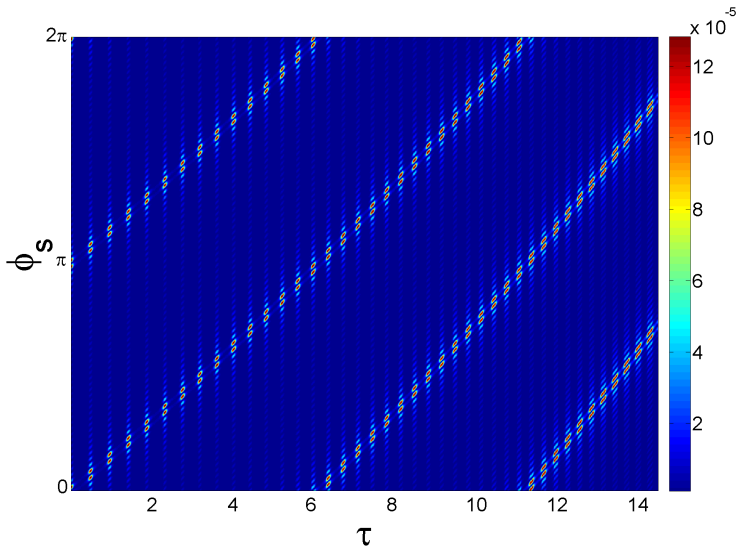

Figure 3.9: Color map of the field intensity of the resonator at $\theta = \pi/2$ and $0 \leq \phi_s \leq 2\pi$ as a function of time. Brighter tone correspond to larger intensity of the field.

environment, which will induce thermal fluctuations of the particle and also exert a viscous force $\mathbf{F_v} = -M_P \beta d\mathbf{r}_P/dt$. The latter limits angular momentum of the particle to its terminal value $\zeta_{term} \propto \kappa/(\beta T)$, which is reached in time $\tau_{term} \propto (\beta T)^{-1}$. If $\zeta_{term} \gg 1$, which also implies $\tau_{term} \gg 1$, the effect of the drag force can be neglected. However, even if $\zeta_{min} < \zeta_{term} < 1$ ensuring existence of the radial potential well, the drag force can actually play a positive role stabilizing particle's motion against ran-away growth of the orbital momentum. In air at normal pressure $\beta T \approx 1$ so that the stable orbital motion of the particles is possible in moderately rarefied atmosphere with densities just two orders of magnitude less than the ambient value. The initial and/or terminal values of ζ must also be small enough to ensure sufficient depth of the radial potential, U_{rad} compared to the thermal energy. The former can be estimated as $U_{rad} \approx (\Lambda_0/T) \tan^{-1}(\sqrt{1-\zeta^2}/\zeta)$. For the same parameter as before $U_{rad} \sim 10^{-17} J$ which by several orders of magnitude exceeds the thermal energy at room temperature. One also needs to be aware about the attractive Van-der-Waals force, which can play a role for particles orbiting too close to the resonator surface. The energy associated

with this force can be estimated as $10^{-18}J$, so it might have to be taken into account when designing the experiment, but should not preclude the orbital effect from being observed.

Actual observation of these effects is facilitated by the fact that the dynamics of the particle is directly reflected in the properties of the electromagnetic field and can be observed optically. Fig. 3.9 illustrates this point showing time evolution of the surface field distribution of the resonator in it's equatorial plane (as defined in XYZ system). As the particle moves, it drags the field along reflecting, therefore, particle's orbital motion and its angular frequency ζ/T. The flushes of intensity of the field along these trajectories reflect radial oscillations of the particle, while the decreasing intervals between consecutive maxima provides information about angular acceleration of the particle. Polar oscillations result in additional fluctuations of intensities at a different from radial oscillations time scale and, can, therefore, also be inferred from observation of the field.

3.5.1 Scattering

One interesting feature of the azimuthal force is that it's direction can be reversed by choosing a WGM with $m = -L$. Therefore, if particles are scattered off the resonator, they can suffer either an increase of decrease of angular momentum. Some general observations can be made. For co-propagating ($m = L$) particles, there will be an increase in ζ and thus an increase in the centrifugal repulsion. The particle will be pulled outward (toward greater y) as compared to the elastic case. Counter-propagating particles ($m = -L$) have the opposite behavior. Now, for $r > r_0$, the azimuthal force is monotonic decreasing, so an increasing (decreasing) ζ will pull the particle outward (inward), weakening (strengthening) the force. Therefore co-propagating particles will experience a larger change in ζ than counter-propagating particles. In the limit where the change in angular momentum becomes so small that the radial motion is unaffected, this change will be identical for both prorogation directions.

Even if $\Delta\zeta$ is large enough to feedback and modify radial motion, a first order cor-

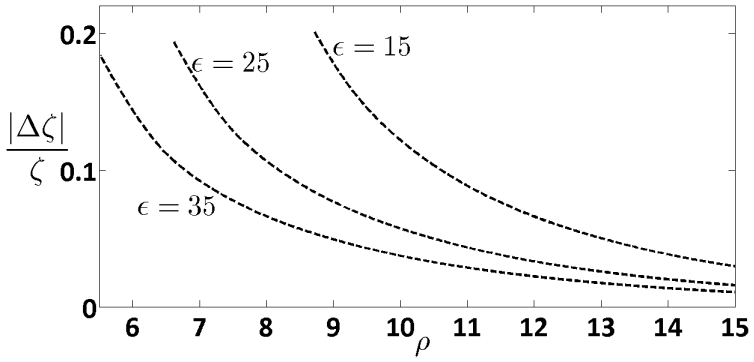

Figure 3.10: Fractional change in angular momentum as a function of impact parameter for co-propagating $m = L$ mode at three energies. Parameters used are $b = 0.0018$, $y_0 = 10$, $p = 0.37$.

rection, $\Delta\zeta^{(0)}$, is calculated by integrating the equations of motion over a trajectory with constant ζ. Based on the preceding discussion, the true change in angular momentum will exceed the first order correction for $m = -L$ and will be less than it for $m = L$. $\Delta\zeta^{(0)}$ is therefore a well-defined asymptote to the actual $\Delta\zeta$. As inelasticity increases, counter-propagating particles will diverge from this asymptote and eventually merge as the maximum is approached.

Numerical integration of the exact equations of motion is shown in Fig. 3.10, where the fractional change in angular momentum $|\Delta\zeta/\zeta|$ for $m = L$ modes as a function of impact parameter for several energies is plotted. The divergence of trajectories with opposite signs of torque is demonstrated in Fig. 3.11.

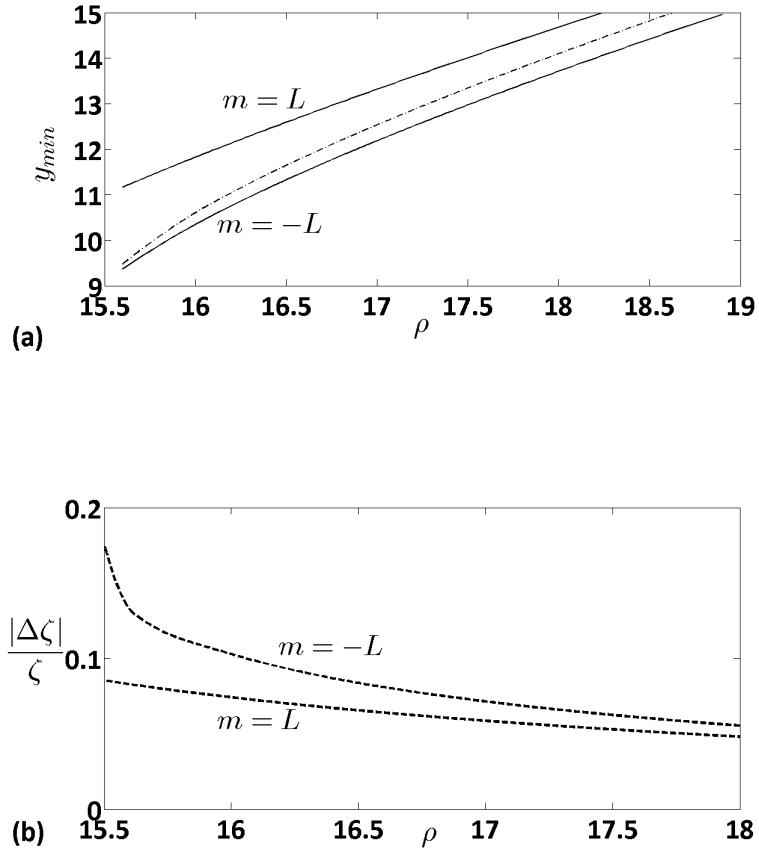

Figure 3.11: (a) Minimum distances for co- and counter-propagating optical modes. The dotted line in the middle is $y_{min}^{(0)}$ neglecting inelasticity. (b) Fractional change in angular momentum for the trajectories in (a). Parameters used are $\epsilon = 10$, $b = 8.56 \cdot 10^{-4}$,$y_0 = 10$, $p = 0.16$.

4. Semi-heuristic derivation of optomechanical interaction

4.1 Force on a Dipole

A *static* polarizable particle has internal energy given by $u = \frac{1}{2}\int \mathbf{E}\cdot\mathbf{D}\ dV$, where $\mathbf{D} = \epsilon_0\mathbf{E} + \mathbf{P}$ and the integral runs over the volume of the particle. $\mathbf{E}$ here refers to the total field, and is comprised of the field of the particle itself in addition to the initial field which polarizes the particle. This latter contribution is labeled $\mathfrak{E}$. This is the field which exists in the absence of the particle, and is assumed to be produced by some external charge distribution that remains unchanged upon introduction of the particle. The quantity $u - \frac{1}{2}\int \epsilon_0|\mathfrak{E}|^2\ dV$ represents the additional energy required to polarize the particle. From this expression is derived the change in internal energy due to a small variation of $\mathfrak{E}$: $\delta u = \int \mathbf{P}\cdot\delta\mathfrak{E}\ dV$. The force is determined by considering δu due to an infinitesimal translation of the particle, $\delta\mathbf{r}_p$. In such a case $\delta\mathfrak{E} = (\delta\mathbf{r}_p\cdot\nabla)\mathfrak{E}$, and $\delta u = -\delta\mathbf{r}_p\cdot\int(\mathbf{P}\cdot\nabla)\mathfrak{E}\ dV$. The total force on the particle is then $\mathbf{F} = \int(\mathbf{P}\cdot\nabla)\mathfrak{E}\ dV$. If $\mathfrak{E}$ is approximately constant over the dimensions of the particle (the definition of a static induced dipole), it can be taken out of the integral, giving $\mathbf{F} = (\mathbf{p}\cdot\nabla)\mathfrak{E}$, where the dipole moment $\mathbf{p} = \int \mathbf{P}\ dV$. Since the particle was assumed to be linear, $\mathbf{p} = \alpha\mathfrak{E}$. By means of vector identities the force can be written:

$$\mathbf{F} = \frac{1}{2}\alpha\nabla|\mathfrak{E}|^2 \tag{4.1}$$

This permits the polarization energy to be interpreted as a potential energy of the particle, giving rise to a conservative force:

$$\mathbf{E}_p = \frac{1}{2}\alpha|\mathfrak{E}|^2 \tag{4.2}$$

An alternative derivation which is commonly encountered is based on a model of an electric dipole as a system of equal and opposite charges $\pm q$, separated by some small, ultimately

infinitesimal distance d. Textbooks usually employ this model to determine the force on a permanent dipole. Instantaneously, an induced dipole of the type discussed here can certainly be modeled as a system of equal and opposite charges. The dipole is assumed to be placed in some external field $\tilde{\mathbf{E}}$, so that $\mathbf{p} = \alpha\tilde{\mathbf{E}}$. We make no demands on $\tilde{\mathbf{E}}$ other than that $\mathbf{p}$ be defined self consistently with it. In particular, $\tilde{\mathbf{E}}$ may be dependent on the dipole itself. For example, if the external field $\tilde{\mathbf{E}}$ is due to charges on a conductor, the presence of the dipole will alter the charge distribution and thus $\tilde{\mathbf{E}}$. We make this explicit by writing $\tilde{\mathbf{E}} = \tilde{\mathbf{E}}(\mathbf{r}, \mathbf{r}_p)$, where $\mathbf{r}$ and $\mathbf{r}_p$ are respectively a field point and the position vector of the particle. The total force is derived by considering the Coulombic force at each end: $\mathbf{F} = q\left[\tilde{\mathbf{E}}(\mathbf{r}_p + \mathbf{d}/2, \mathbf{r}_p) - \tilde{\mathbf{E}}(\mathbf{r}_p - \mathbf{d}/2, \mathbf{r}_p)\right]$. By taking the limit $|\mathbf{d}| \to 0$, keeping $|\mathbf{p}| = q|\mathbf{d}|$ constant, the force derived in this case is:

$$\mathbf{F} = \left[(\mathbf{p} \cdot \nabla_{\mathbf{r}})\tilde{\mathbf{E}}\right]_{\mathbf{r}=\mathbf{r}_p} \tag{4.3}$$

Where $\nabla_{\mathbf{r}}$ refers to a gradient with respect to field coordinates $\mathbf{r}$. This is just like the force found from the first derivation, except we are being very careful to take the gradient with respect to a *field point*, $\mathbf{r}$, and then evaluate this field gradient at the position of the particle, $\mathbf{r} = \mathbf{r}_p$. One can similarly transform this expression to: $\mathbf{F} = \frac{1}{2}\alpha\nabla_{\mathbf{r}}|\tilde{\mathbf{E}}(\mathbf{r}, \mathbf{r}_p)|^2 \;|_{\mathbf{r}=\mathbf{r}_p}$. The crucial difference is that this is no longer a total derivative of some function of $\mathbf{r}_p$, and there is no associated conserved energy.

The physical significance of this pseudo-gradient is that, while an actual displacement of the particle alters the field distribution, the force it experienced depends only on the instantaneous field. Both approaches give the same result if $\tilde{\mathbf{E}}$ is independent of the particle. We use the notation $\tilde{\nabla}$ to denote the pseudo-gradient operation.

Now consider a dipole in a time harmonic field. The oscillating dipole moment creates a current density $d\mathbf{p}/dt$, giving rise to a magnetic force. The total Lorentz force on the particle for unmodified incident fields $\mathfrak{E}, \mathfrak{B} = -i/\omega\nabla\times\mathfrak{E}$ can be written $\mathbf{F} = (\mathbf{p}\cdot\nabla)\mathfrak{E} + d\mathbf{p}/dt\times\mathfrak{B}$. By

means of vector identities and Maxwell's equation's, the time average force for complex fields can be expressed by [41]: $\langle \mathbf{F} \rangle = \frac{1}{4}\mathcal{R}e[\alpha]\nabla|\mathfrak{E}|^2 + \frac{1}{2}\mathcal{I}m[\alpha]\left(\omega\mathcal{R}e[\mathfrak{E}^* \times \mathfrak{B}] + \mathcal{I}m[(\mathfrak{E}^* \cdot \nabla)\mathfrak{E}]\right)$. With the understanding of how to properly deal with gradients, the time averaged force for the general case $\mathbf{E} = \mathbf{E}(\mathbf{r}, \mathbf{r}_p)$ is obtained by substituting $\mathfrak{E}, \mathfrak{B}, \nabla$ with $\mathbf{E}, \mathbf{B}, \tilde{\nabla}$ respectively. For a standard dipole particle with radius R_p, refractive index n_p, and polarizability $\alpha = 4\pi\epsilon_0(\alpha_0 + \frac{2}{3}ik^3|\alpha_0|^2)$, where $\alpha_0 = R_p^3(n_p^2 - 1)/(n_p^2 + 2)$, the force can be re-written $\langle \mathbf{F} \rangle = \tilde{\nabla}\langle u \rangle + \sigma c \langle \mathbf{g} \rangle + \sigma c \frac{\epsilon_0}{2\omega}\mathcal{I}m[(\mathbf{E}^* \cdot \tilde{\nabla})\mathbf{E}]$, where $\langle u \rangle$ is the average polarization energy of the dipole $\langle u \rangle = \frac{1}{2}\mathcal{R}e[\frac{1}{2}\mathbf{p} \cdot \mathbf{E}]$, σ is the scattering cross section of a dipole $\sigma = \mathcal{I}m[\alpha]k/\epsilon_0$, $\langle \mathbf{g} \rangle$ is the average momentum density in the wave $\langle \mathbf{g} \rangle = \frac{1}{2}\mathcal{R}e[\epsilon_0 \mathbf{E} \times \mathbf{B}]$ and c is the speed of light.

4.1.1 Hamiltonian Formalism for Frequency Shifts

The Hamiltonian structure of electromagnetic modes provides a connection between frequency shifts and associated forces. If a particle is introduced into the field adiabatically, it's energy will shift by $\delta E = E_p$, with E_p given by Eq. 4.2. By Eq. 2.87, the frequency will also shift with the adiabatic invariant $I = E/\omega$ remaining constant. This has the interpretation that average photon number is conserved. The frequency shift will be:

$$\delta\omega = \frac{\omega\delta E}{E} = \frac{E_p}{N\hbar} \tag{4.4}$$

The force on the particle has already been shown to be equal to the variation of energy per variation of the particle coordinate. Thus, writing $\delta E = F\delta r$, the force is:

$$F = \frac{\delta E}{\delta r} = N\hbar\frac{\partial\delta\omega}{\partial r} \tag{4.5}$$

This force is identified with the gradient force derived above, and is seen simply be the derivative of mode energy with respect to particle coordinate.

4.1.2 Particle outside Resonator

These simple results are used extensively in the literature on optomechanics. Strictly speaking they are only valid for a particle within a lossless resonator. However, the case of a particle outside a resonator is qualitatively different. In this case, the field outside the resonator vanishes in the $\Gamma \to 0$ limit, and there will be no coupling. One way to deal with this is to extend the mode region outside of the cavity. The external fields will differ from internal by a factor Γ, to which $\delta E = E_p$ will be proportional. However, we would like to understand the behavior of the frequency shift in a more general way that encapsulates the effect of modal decay. Since the Hamiltonian of the mode includes only the energy within the sphere, we cannot assume that the variation of energy induced by the particle is equal to it's polarization energy. We do know however, that the particle is radiating and therefore the field does work on it equal to the rate of energy loss by particle radiation, $W = \mathbf{j} \cdot \mathbf{E}$. By the reciprocity theorem, $\mathbf{j}_1 \cdot \mathbf{E}_2 = \mathbf{j}_2 \cdot \mathbf{E}_1$ [42], the field scattered by the particle does an equal amount of work on the surface currents circulating in the walls of the resonator. The real and imaginary parts of $\mathbf{j} \cdot \mathbf{E}$ can be interpreted as in Sec. 2.1.8. Thus, the particle induces a variation in the power radiated by the resonator $\delta P = (1/2)\mathcal{R}e\ \mathbf{j} \cdot \mathbf{E}^* = (1/2)\omega\mathcal{I}m\ \alpha|\mathbf{E}|^2$, leading to a change in width:

$$\frac{\delta\Gamma}{\Gamma} = \frac{\delta P}{P} \tag{4.6}$$

If the field of the particle does work on the surface currents in the walls of the resonator equal to $-\omega\mathcal{I}m\alpha|\mathbf{E}|^2/2$, then there is a corresponding stored energy $\mathcal{R}e\alpha|\mathbf{E}|^2/4$. Therefore $\delta\omega/\delta\Gamma = \mathcal{R}e[\alpha]/\mathcal{I}m[\alpha]$. This gives $\delta\omega$ as:

$$\frac{\delta\omega}{\omega} = \frac{1}{\mathcal{I}m[\alpha]}\frac{\delta P}{P} \tag{4.7}$$

4.1.3 Particle Modifying Cavity Field

Concerning the gradient force, the Hamiltonian approach assumes that δE is small, while the electromagnetic approach assumes that a perturbing particle does not alter the field distribution of the cavity mode. What about if this condition is not satisfied? This can occur when there are multiple modes in the cavity with different phases, so that even if the coupling to one is small, the resultant field distribution is altered. Additionally, for a driven cavity with resonant amplitude Eq. 2.57, the steady state amplitude or photon number will shift with the frequency, so the action is not necessarily invariant. However if ω_0 changes slowly over the scale of both ω_0 and Γ_0 the field can be assumed to always be in the steady state with energy:

$$E = \frac{1}{y^2+1} E_0 \tag{4.8}$$

where:

$$y = \frac{\omega - \omega_0}{\Gamma_0} \tag{4.9}$$

and E_0 is the energy when $\omega = \omega_l^{(0)}$. Eq. 4.8 can be regarded as an effective Hamiltonian which reproduces the correct oscillator equations when time derivatives of the amplitude are neglected. When calculating the generalized force on the particle from this Hamiltonian, the amplitude factor is treated as a function of time, not as an explicit function of ω_0. The reason for this is the causality requirement that the the amplitude should not change until after the frequency shift. In other words, since the field evolves with the particle, there is a difference between a physical and virtual displacement of the particle. The force is determined by the virtual displacement, while the change in amplitude does not occur until the particle physically starts to move. The force is thus:

$$\frac{dp_r}{dt} = \frac{1}{y^2+1} \frac{d}{dr_p} E_0 \tag{4.10}$$

Now consider that the cavity consists of several almost degenerate modes, so that the Hamiltonian is of the form:

$$H = \sum_j H_j = \sum_j I_j \omega_j \tag{4.11}$$

Assume that the the amplitudes of these modes are related by some group transformation, such as a rotation:

$$a_i = \sum_j T_{ij}(\xi) a_j \tag{4.12}$$

where T is some transformation. Suppose also that T depends on some coordinate ξ of the particle, which is coupled via interaction Hamiltonian:

$$\delta H = \sum_j \delta H_j = \sum_j c_j H_j \tag{4.13}$$

We look for the adiabatic evolution among the steady states. If the coupling constants c_j of the interaction Hamiltonian do not depend on the coordinates of this transformation, the frequency shifts $\delta\omega_j/\omega_j = \delta H_j/H_j$ are independent of this coordinate. Motion of the particle along this coordinate simply changes the relative strengths of each mode, but do not change their frequencies. A force can still be exerted on the particle due to modal coupling however, which leads to movement of the ξ coordinate and thus a change of the transformation T. To follow the path of the particle we determine this force at each position and continuously re-diagonalize the Hamiltonian. Once again, the different steady state amplitudes Eq. 4.12 are causally disconnected, since the particle must first break the steady state corresponding to $\xi(t)$, allowing the system to respond and relax into the new steady state at $\xi(t+dt) = \xi + d\xi$. Due to the group transformation property Eq. 4.12, the amplitude of one mode will appear as a source in the time evolution equation for another mode. The forcing appears when the steady state Hamiltonian of the system for a given ξ is expressed in coordinates corresponding to $\xi + d\xi$ where it may in general be non-diagonal. If t_{ij} is the infinitesimal generator of T, the mode coefficients become coupled as $a_i = a_i + d\xi \sum_j t_{ij} a_j$, representing a passive

transformation. The steady state is achieved by re-defining the a_i so as to cancel out the first transformation and assume steady state form. The latter step corresponds to physical motion of the particle. Thus, we determine the force on the particle from the change of δH upon rotation, which is of course just the generalized force.

$$\frac{dp_{xi}}{dt} = -\frac{\partial H}{\partial \xi} \tag{4.14}$$

This force will also be non-conservative since it continually re-adjusts itself with the motion of the particle. We have seen that the force is non-conservative in the sense that it is not derivable from a total derivative of a function, which stems from the fact that the driving source renormalizes the amplitude I. Since the field distribution is not static, but depends on the perturbing particle, this force can obviously not be identified with the "gradient force", which assumes this. Thus, the operation is achieved by taking the spatial gradient of the field at a specific instant of time. As long as the field is expanded in quasi-normal modes, the distinction between gradient and psuedo-gradient is clear: one takes the derivative of the spatial mode functions while leaving the coefficients constant. Thus, the derivative Eq. 4.10 is clearly identical to this operation. Similarly, the derivative with respect to angular coordinates is simply the change of the function due to infinitesimal rotation, which is exactly like the operation of Eq. 4.10 where the coordinate rotation at constant coupling coefficients.

4.1.4 Point-Dipole WGM Interaction

The preceding method will be applied to the interaction of a point dipole with a spherical microcavity that it is positioned outside of it. The resonator is excited to WGM of mode $l = L, m = L, \sigma = \sigma_0$ defined in a coordinate system $X'Y'Z'$ and maintained in the steady state by a driving field. The field inside the sphere is $\mathbf{E}_{int} = a_{int}\mathbf{J}_{L,L,\sigma_0}$ while outside it is $\mathbf{E}_{scat} = a_{scat}\mathbf{H}_{L,L,\sigma_0}$. A subwavelength particle is brought into the evanescent

region of the sphere. To begin with application of Eq. 4.6, we need the power loss induced by introduction of the particle. The average power loss is $\frac{1}{2}\mathcal{R}e\int \mathbf{J}\cdot\mathbf{E}^*$. With $\mathbf{p}=\alpha\mathbf{E}$ and $\int \mathbf{J}\ dV = \partial p/\partial t$, this term becomes:

$$\frac{1}{2}Re\int \mathbf{J}\cdot\mathbf{E}^* = Re\frac{i\omega\alpha}{2}|\mathbf{E}|^2 = \frac{-\omega Im[\alpha]}{2}|\mathbf{E}|^2 \tag{4.15}$$

Interaction with a point dipole is most conveniently analyzed when the electric field of the resonator is expressed in a system XYZ where the particle lies along the Z axis. If the position of the particle in the $X'Y'Z'$ system is $\mathbf{r}_p=(r_p,\theta_p,\phi_p)$, the new coordinate system is obtained by rotating $X'Y'Z'$ by Euler angles $\alpha=\phi_p$ and $\beta=\theta_p$. The coefficients of the WGM in this system are $c_{L,m,\sigma}=\delta_{\sigma,\sigma_0}\delta_{l,L}c_m$, where:

$$c_m = \frac{i}{y_0+i}D^{(L)}_{m,L}(0,-\theta_p,-\phi_p) \tag{4.16}$$

According to Eq.2.39, the power radiated by the resonator is:

$$P = \frac{c\epsilon_0 E_0^2}{2k^2}\sum m\frac{1}{y_0^2+1}|D^{(L)}_{m,L}(0,-\theta_p,-\phi_p)|^2 = \sum_m P_m \tag{4.17}$$

The electric field at a point along the Z axis, $\mathbf{E}(\mathbf{r})=\mathbf{E}(r\hat{\mathbf{z}})$ is

$$\mathbf{E}(r\hat{\mathbf{z}}) = E_0\sqrt{\frac{L}{4\pi}}\begin{cases} h_L^{(1)}(kr)\left(c_{-1}\hat{\xi}_+ + c_1\hat{\xi}_-\right) & \sigma_0=M \\ -i\sqrt{2}L\dfrac{h_L^{(1)}(kr)}{kr}c_0\hat{z} + \dfrac{[krh_L^{(1)}]'}{kr}\left(c_{-1}\hat{\xi}_+ - c_1\hat{\xi}_-\right) & \sigma_0=E \end{cases} \tag{4.18}$$

Using Eq. 4.15 and Eq. 4.18, the work done due to introduction of the particle is:

$$\delta P = \sum_{m=-1,0,1}\delta_{P_m}P_m \tag{4.19}$$

where:

$$\delta_{P_m} = \frac{Lk^3}{4\pi\epsilon_0} \begin{cases} |h_L(kr_p)|^2 & \sigma_0 = M,\ m = \pm 1 \\ \dfrac{|[kr_p h_L(kr_p)]'|^2}{k^2 r_p^2} & \sigma_0 = E,\ m = \pm 1 \\ 2L^2 \dfrac{|h_L(kr_p)|^2}{k^2 r_p^2} & \sigma_0 = E,\ m = 0 \\ 0 & |m| > 1 \end{cases} \tag{4.20}$$

Using Eq. 4.6, the broadening of each mode, $\delta\Gamma_m$ is:

$$\delta\Gamma_m = \Gamma_m \delta_{P_m} \tag{4.21}$$

Then, by Eq. 4.7, we have the frequency shift:

$$\delta\omega_m = \frac{\mathcal{R}e\ \alpha}{\mathcal{I}m\ \alpha}\Gamma_m \delta_{P_m} \tag{4.22}$$

Given frequency and width changes, the amplitude of the driven modes re-adjust. The factor $(y+i)^{-1}$ becomes modified by the replacement $y = (\omega - \omega_0)/\Gamma \to y_m = (\omega - \omega_m)/\Gamma_m$. The "psuedo-gradient" force on the particle in the radial direction is achieved by differentiating the modes functions but not the amplitude coefficients. This is:

$$F_r = \frac{\mathcal{R}e[\alpha]L}{16\pi} \begin{cases} |c_{-1}|^2 \dfrac{d}{dr}|h_L^{(1)}(kr)|^2 + |c_1|^2 \dfrac{d}{dr}|h_L^{(1)}(kr)|^2 & \sigma_0 = M \\ |c_0|^2 \dfrac{d}{dr}|\dfrac{[krh_L^{(1)}]'}{kr}|^2 + |c_{-1}|^2 \dfrac{d}{dr}|\dfrac{h_L^{(1)}(kr)}{kr}|^2 + |c_1|^2 \dfrac{d}{dr}|\dfrac{h_L^{(1)}(kr)}{kr}|^2 & \sigma_0 = E \end{cases} \tag{4.23}$$

where the normalization has been set to $E_0 = 1$. The "psuedo-gradient" force in the polar direction is given by Eq. 4.14 with the transformation Eq. 2.26 with $\epsilon_x = d\theta_p$:

$$F_\theta^{(pg)} = -\frac{d\delta H}{d\theta_p} = \frac{\mathcal{R}e[\alpha]L^2}{16\pi r \sin\theta_p}\mathcal{R}e\ \left(c_1(c_0^* - c_2^*) - c_{-1}(c_0^* - c_{-2}^*)\right) \tag{4.24}$$

The presence of c_2 modes comes from the infinitesimal generator, Eq. 2.26, which couples modes differing by one m index. The "psuedo-gradient" force in the azimuthal direction is achieved with the rotation angle $\epsilon_y = d\phi_p$:

$$F_\phi^{(pg)} = -\frac{d\delta H}{d\phi_p} = \frac{\mathcal{R}e[\alpha]L^2}{16\pi r_p \sin\theta_p}\mathcal{I}m\ \left(c_1(c_0^* + c_2^*) - c_{-1}(c_0^* + c_{-2}^*)\right) \tag{4.25}$$

The "scattering" force is:

$$\sigma c\mathbf{g} = \frac{\mathcal{I}m[\alpha]L^2}{16\pi r_p \sin\theta_p}\mathcal{I}m\ \left(c_1 c_0^*\hat{\theta} - c_{-1}c_0^*\hat{\phi}\right) \tag{4.26}$$

4.2 Summary and Outlook

The theory presented here discusses the interaction of a subwavelength particle with a spherical WGM resonator from several perspectives. Explicit calculations of the full scattered field of the resonator-particle system are carried out using multi-sphere Mie theory and provide exact results within the approximation that the particle can be treated as a small sphere. The forces exerted on the particle by the field are derived and used to determine the trajectories of the particle. These results show that the ideal Mie resonance is not strictly speaking, "split". Rather, certain degenerate modes are shifted while others remain unaffected. For TM polarized modes there are two shifted resonances, with the extra corresponding to the interaction of the particle with the radial component of the field.

This two-sphere scattering system is a rare analytically solvable model. To further elucidate the main conceptual points of this interaction, the fields and forces are also calculated from a semi-heuristic model which treats the particle as a perturbation that couples ordinarily degenerate modes of the resonator. This second derivation reproduces the exact results in a simpler way. However, this heuristic approach differs from the usual gradient/scattering force paradigm. The relationship between frequency shift, gradient force, and conservation of average photon number arises because the evolution of the field occurs over a time scale

much longer than it's oscillation period. This condition can be satisfied even when energy is not conserved, as for example with a damped, driven mode with a frequency dependant resonant amplitude discussed here. In this case the photon number is still conserved even though the force is non-conservative. This is due to the fact that the force on the particle is generated by the instantaneous fields, which then re-adjust as the particle moves. The scattering force is also found to differ from that which would be expected for an unmodified resonator, in that it has a contribution proportional to the real part of the particle polarizability. This is due to the presence of a field gradient in the azimuthal direction when the resonator modes become modified. This force is non-conservative as well, because the field adjusts and re-establishes this gradient as the particle moves. This heuristic derivation might be of value in extending the present results to other resonators with axial symmetry, since the principle assumption of the theory is that different modes couple as the particle rotates. In particular, it is expected that for other WGM resonators the azimuthal force should also have a gradient component.

Trajectories of the particle are calculated within the adiabatic regime where the field is always in the steady state. If the particle moves significantly over the time scale of the modal decay of the resonator, this assumption breaks down. In such a case one would have to solve for the dynamics of particle and field self-consistently. Relativistic effects are also not considered in the present model. Such effects can be expected to play a role if the doppler frequency shift due to the moving particle is comparable to the width of the mode.

LITERATURE CITED

[1] K. J. Vahala. Optical microcavities. *Nature*, 424:839–845, 2003.

[2] M. L. Gorodetsky, A. D. Pryamikov, and V. S. Ilchenko. Rayleigh scattering in high-q microspheres. *J. Opt. Soc. Am. B*, 17(6):1051–1057, 2000.

[3] D. S. Weiss, V. Sandoghdar, J. Hare, V. Lefèvre-Seguin, J.-M. Raimond, and S. Haroche. Splitting of high-q mie modes induced by light backscattering in silica microspheres. *Opt. Lett.*, 20(18):1835–1837, 1995.

[4] B. E. Little, J. P. Juha-Pekka Laine, and S. T. Chu. Surface-roughness-induced contradirectional coupling in ring and disk resonators. *Opt. Lett.*, 22(1):4–6, 1997.

[5] T. J. Kippenberg, S. M. Spillane, and K. J. Vahala. Modal coupling in traveling-wave resonators. *Opt. Lett.*, 27(19):1669–1671, 2002.

[6] M. Borselli, T. Johnson, and O. Painter. Beyond the rayleigh scattering limit in high-q silicon microdisks: theory and experiment. *Opt. Express*, 13(5):1515–1530, 2005.

[7] O. Romero-Isart, A. C. Pflanzer, M. L. Juan, R. Quidant, N. Kiesel, M. Aspelmeyer, and J. I. Cirac. Optically levitating dielectrics in the quantum regime: Theory and protocols. *Phys. Rev. A*, 83:013803, Jan 2011.

[8] Kirk A. Fuller. Optical resonances and two-sphere systems. *Applied Optics*, 30:4716, 1991.

[9] K. A. Fuller and G. W. Kattawar. Consummate solution to the problem of classical electromagnetic scattering by an ensemble of spheres. i: Linear chains. *Opt. Lett.*, 13(2):90–92, Feb 1988.

[10] K. A. Fuller and G. W. Kattawar. Consummate solution to the problem of classical electromagnetic scattering by an ensemble of spheres. ii: Clusters of arbitrary configuration. *Opt. Lett.*, 13(12):1063–1065, Dec 1988.

[11] Yu lin Xu. Electromagnetic scattering by an aggregate of spheres. *Appl. Opt.*, 34(21):4573–4588, Jul 1995.

[12] L. Deych and J. Rubin. Rayleigh scattering of whispering gallery modes of microspheres due to a single dipole scatterer. *Phys. Rev. A*, 80:061805, Dec 2009.

[13] J. T. Rubin and L. Deych. *Ab initio* theory of defect scattering in spherical whispering-gallery-mode resonators. *Phys. Rev. A*, 81:053827, May 2010.

[14] A. Ashkin, J. M. Dziedzic, J. E. Bjorkholm, and Steven Chu. Observation of a single-beam gradient force optical trap for dielectric particles. *Opt. Lett.*, 11(5):288–290, May 1986.

[15] A. Ashkin. Acceleration and trapping of particles by radiation pressure. *Phys. Rev. Lett.*, 24:156–159, Jan 1970.

[16] D. J. Wilson, C. A. Regal, S. B. Papp, and H. J. Kimble. Cavity optomechanics with stoichiometric sin films. *Phys. Rev. Lett.*, 103:207204, Nov 2009.

[17] Oriol Romero-Isart, Mathieu L Juan, Romain Quidant, and J Ignacio Cirac. Toward quantum superposition of living organisms. *New Journal of Physics*, 12(3):033015, 2010.

[18] P. F. Barker and M. N. Shneider. Cavity cooling of an optically trapped nanoparticle. *Phys. Rev. A*, 81:023826, Feb 2010.

[19] Zhang-qi Yin, Tongcang Li, and M. Feng. Three-dimensional cooling and detection of a nanosphere with a single cavity. *Phys. Rev. A*, 83:013816, Jan 2011.

[20] T. J. Kippenberg and K. J. Vahala. Cavity optomechanics: Back-action at the mesoscale. *Science*, 321(5893):1172–1176, 2008.

[21] S. Arnold, D. Keng, S. I. Shopova, S. Holler, W. Zurawsky, and F. Vollmer. Whispering gallery mode carousel – a photonic mechanism for enhanced nanoparticle detection in biosensing. *Opt. Express*, 17(8):6230–6238, Apr 2009.

[22] J. T. Rubin and L. I. Deych. Optical forces due to spherical microresonators and their manifestation in optically induced orbital motion of nanoparticles. *Phys. Rev. A*, 84:023844, Aug 2011.

[23] J. T. Rubin and L. Deych. On optical forces in spherical whispering gallery mode resonators. *Opt. Express*, 19(22):22337–22349, Oct 2011.

[24] J. A. Stratton. *Electromagnetic theory*. McGraw-Hill Book Company, New York and London, 1941.

[25] J. D. Jackson. *Classical Electrodynamics*. John Wiley & Sons, Inc., 1999.

[26] Eugen Merzbacher. *Quantum Mechanics*. John Wiley & Sons, Inc, New York, 2005.

[27] M. I. Mishchenko, L. D. Travis, and A. A. Lacis. *Scattering, Absorption and Emission of Light by Small Particles*. Cambridge University Press, Cambridge, 2002.

[28] K.T. Kim. Symmetry relations of the translation coefficients of the spherical scalar and vector multipole fields. *Progress in Electromagnetics Research*, 48, 2004.

[29] Vadim A. Markel. Pole expansion of the lorenz-mie coefficients. *Journal of Nanophotonics*, 4:041555, 2010.

[30] C. C. Lam, P. T. Leung, and K. Young. Explicit asymptotic formulas for the positions, widths, and strengths of resonances in mie scattering. *J. Opt. Soc. Am. B*, 9(9):1585–1592, Sep 1992.

[31] Herbert Goldstein. *Classical Mechanics*. Addison Wesley, Masschusets, 1950.

[32] L.D. Landau and E.M. Lifshitz. *Mechanics*. Elsevier, 1994.

[33] David J. Griffiths. *Introduction to Electrodynamics*. Pearson - Addison Wesley, New Jersey, 1999.

[34] Jun Chen, Jack Ng, Shiyang Liu, and Zhifang Lin. Analytical calculation of axial optical force on a rayleigh particle illuminated by gaussian beams beyond the paraxial approximation. *Phys. Rev. E*, 80:026607, Aug 2009.

[35] P. C. Chaumet and M. Nieto-Vesperinas. Time-averaged total force on a dipolar sphere in an electromagnetic field. *Opt. Lett.*, 25(15):1065–1067, Aug 2000.

[36] A. Mazzei, S. Götzinger, L. de S. Menezes, G. Zumofen, O. Benson, and V. Sandoghdar. Controlled coupling of counterpropagating whispering-gallery modes by a single rayleigh scatterer: A classical problem in a quantum optical light. *Phys. Rev. Lett.*, 99(17):173603, 2007.

[37] M. Abramowitz and I Stegun. *Handbook of Mathematical Functions with Formulas, Graphs and Mathematical Tables*. US Government Printing Office, 1964.

[38] Yoshiko Hara, Takashi Mukaiyama, Kenji Takeda, and Makoto Kuwata-Gonokami. Heavy photon states in photonic chains of resonantly coupled cavities with supermonodispersive microspheres. *Phys. Rev. Lett.*, 94(20):203905, 2005.

[39] C. P. Dettmann, G. V. Morozov, M. Sieber, and H. Waalkens. Directional emission from an optical microdisk resonator with a point scatterer. *Europhysics Letters*, 82:34002–+, May 2008.

[40] D. E. Chang, C. A. Regal, S. B. Papp, D. J. Wilson, J. Ye, O. Painter, H. J. Kimble, and P. Zoller. Cavity opto-mechanics using an optically levitated nanosphere. *Proceedings of the National Academy of Sciences*, 107(3):1005–1010, 2010.

[41] Vance Wong and Mark A. Ratner. Explicit computation of gradient and nongradient contributions to optical forces in the discrete-dipole approximation. *J. Opt. Soc. Am. B*, 23(9):1801–1814, Sep 2006.

[42] L.D. Landau, E.M. Lifshitz, and L.P. Pitaevskii. *Electrodynamics of Continuous Media*. Elsevier, 1984.